ABSTRACT

Total Electron Scattering Cross Sections of Tetrafluoromethane, Trifluoromethane, Hexafluoroethane, and Octafluorocyclobutane in the Energy Range 0.10 to 4.50 keV

Prasanga D. Palihawadana, M.S.

Mentor: Wickramasinghe Ariyasinghe, Ph.D.

The total electron scattering cross sections of Tetrafluoromethane (CF4), Trifluoromethane (CHF_3), Hexafluoroethane (C_2F_6), and Octafluorocyclobutane (c-C_4F_8) are measured in the energy range 0.10 to 4.50 keV using the linear transmission technique. The measured experimental cross sections are compared with other experimental and theoretical cross sections available in the literature. A simple empirical formula is also developed by using the present measurements to predict the cross sections of linear fluorocarbons as a function of the electron energy and the number of atoms in the target molecule. This empirical formula is used to calculate the total cross sections of linear fluorocarbons in the energy range 0.30 to 3.50 keV. Those empirically calculated cross sections are compared to the present experimental cross sections and other experimental and theoretical cross sections available in the literature.

Total Electron Scattering Cross Sections of Tetrafluoromethane, Trifluoromethane, Hexafluoroethane, and Octafluorocyclobutane in the Energy Range 0.10 to 4.50 keV

by

Prasanga D. Palihawadana

A Thesis

Approved by the Department of Physics

_____

Gregory A. Benesh, Ph.D., Chairperson

Submitted to the Graduate Faculty of
Baylor University in Partial Fulfillment of the
Requirements for the Degree
of
Master of Science

Approved by the Thesis Committee

_____

Wickramasinghe M. Ariyasinghe, Ph.D., Chairperson

_____

Kenneth T. Park, Ph.D.

_____

Lorin S. Matthews, Ph.D.

_____

John A. Olson, Ph.D.

Accepted by the Graduate School
December 2008

_____

J. Larry Lyon, Ph.D., Dean

Page bearing signatures is kept on file in the Graduate School.

TABLE OF CONTENTS

LIST OF FIGURES

LIST OF TABLES

ACKNOWLEDGMENTS

The author would like to express his gratitude to his research supervisor and the chairman of the thesis committee, Dr. Wickramasinghe Ariyasinghe for his continuous support, encouragement and guidance throughout this work. I'd also like to express my sincere appreciations to my thesis committee, Dr. Lorin S. Matthews, Dr. Kenneth T. Park, and Dr. John A. Olson, for their time and valuable suggestions. Finally, I want to thank the faculty and staff of the Department of Physics, Graduate School and the Baylor University for giving me the opportunity of pursuing studies at Baylor.

The author would like to dedicate this work to his loving parents and wife.

CHAPTER ONE

Introduction

1.1. Electron-Atom/Molecule Collisions

Studies of electron-atom (and electron-molecule) collisions play a major role in the understanding of electronic and chemical properties and the internal structure of those atoms and molecules. For more than a century, with the discovery of the electron by J.J. Thomson in 1897, scientists had being using electrons to investigate properties of atoms (or molecules) of interest [1]. Among those studies, electron scattering in gas phase, where a beam of energetic electrons passes through a target gas, is considered as one of the most important phenomena and hence one of the most widely studied area in Atomic and Molecular Physics. Here a beam of energetic electrons is passed through the target gas creating various kinetic processes, due to interactions of electrons with gas atoms or molecules. These processes can be divided into inelastic collisions and elastic collisions depending on the type of the interaction involved. Inelastic collisions occur when there is a loss in kinetic energy of the primary electron beam while those processes with no kinetic energy loss in primary electrons are called elastic collisions. Although during elastic collisions electrons can lose a part of its energy due to momentum transfer, this energy loss is significantly smaller since it is proportional to the ratio of electron mass to molecular mass. Therefore, in general, these processes are considered as elastic collisions. The kinetic energy loss in inelastic collisions is mainly due to the ionization of the target molecule, excitation of the target molecule, and other internal processes

resulted from electron-molecule collisions. The probability of scattering due to either of these two processes can be specified by their respective cross sections.

1.2. Total Electron Scattering Cross Section (TCS)

The total electron scattering cross section (TCS) is defined as the total probability of scattering an energetic electron as it penetrates through a medium - in this study the target gas. Alternatively, the total electron scattering cross section can be considered as a measure of the "effective surface area" of the target atom or molecule presented to an energetic beam of electrons. Therefore TCS is expressed in the units of area - m^2 in this study.

In terms of different types of kinetic energy processes involved, the total electron scattering cross section *(*σ_T) is defined as the sum of the cross sections of all possible interactions between electrons and target atoms or molecules. This can be expressed as an equation in the following form.

$$\sigma_T = \sigma_t^{El} + \sigma_t^{In} \tag{1.1}$$

Here, σ_t^{El} is the total elastic scattering cross section while σ_t^{In} is the total inelastic scattering cross section. The inelastic scattering of electrons by an atom or a molecule could be due to any of the several internal processes such as ionization, excitation, rotation, vibration, or electron attachment of that atom or molecule. Therefore the total inelastic scattering cross section (σ_t^{In}) can be expressed as;

$$\sigma_t^{In} = \sigma_t^{Ion} + \sigma_t^{Exc} + \sigma_t^{Other} \tag{1.2}$$

where, σ_t^{Ion} is the total ionization cross section, σ_t^{Exc} is the total excitation cross section and σ_t^{Other} is the total cross section due to other internal processes of the target atom or molecule.

All of the above mentioned cross sections, total and individual, are important in understanding electron-atom (and electron-molecule) collisions. Although one can measure individual cross sections separately, it has been agreed that the most accurate and reliable measurements can be obtained from direct measurements of total cross section measurements [2]. Also, experimental results show that individual cross section measurements generally carry a larger error compared to the total cross section measurements. It has been observed that the error in total cross section measurements are within the 1-5 % range while those in inelastic cross sections measurements are more than 5% [2].

1.3. Applications of Fluorocarbon Total Electron Scattering Cross Sections

Applications of total electron scattering cross sections are important in a variety of fields in physics, chemistry, biology and even medicine. These applications are ranging from basic sciences, as in astrophysics or atmospheric physics, to real life applications, as in semiconductor-etching or radiation damage. Also it is very important to have reliable experimental cross sections to develop and confirm theoretical models. Since little or no experimental cross sections are available for the condensed phase, gas phase cross sections are often used to estimate condensed phase cross sections. Therefore it is very important to have an accurate set of experimental and theoretical cross sections for the gas phase.

The fluorocarbons used for this study, Tetrafluoromethane (CF4), Trifluoromethane (CHF_3), Hexafluoroethane (C_2F_6), and Octafluorocyclobutane (c-C_4F_8), are widely used for semiconductor etching and hence often referred to as plasma processing gases. Plasma etching is one of the most widely used processes in the semiconductor industry. It is used both for creating semiconductor structures and for developing photoresists. Since most of the new plasma tools operate at low pressure and high plasma densities, the gasses which are used for these processes are highly fragmented. It has been reported that in some cases feedstock gasses disassociate over 90% [3]. Therefore electron scattering cross sections and disassociation cross sections for fragments of these gasses are useful in the development of plasma equipments as well as in the understanding of the mechanisms of plasma processes.

Tetrafluoromethane (CF_4) is a man-made gas and one of the most widely used components of feed gas mixtures. "It serves as a source of reactive species (ions, neutrals, radicals) which are largely responsible for surface reactions in various etching and deposition applications" [4]. Mainly due to no existing (stable) excited states of the CF_4 molecule, it is considered as an ideal source for plasma etching process. CF_4 is also used in pulse power switching, gaseous dielectrics, gas discharges, and host of other applications in physics and chemistry [4]. Although CF_4 is used in all these applications, it is also considered as a greenhouse gas contributing to global warming. To make the matter worst, this has a lifetime of 50 000 years in the atmosphere, thousands of times higher than that of CO_2. Therefore to assess the behavior of this gas in the atmosphere and in the semiconductor industry, it is necessary to have information about its electronic and ionic interactions and its electron collision processes in a wide energy range.

Trifluoromethane (CHF_3) is also used in the semiconductor industry as a plasma processing gas. Since it has a relatively shorter lifetime (250 years) in the atmosphere, CHF_3 is considered as a desirable substitute for CF_4 in some industrial applications [5]. Hexafluoroethane (C_2F_6) is a man-made gas and mainly used in the aluminum industry, in the semiconductor industry, in pulsed power switching gas mixtures, in plasma chemistry and in carbon-13 separation [6]. Like other fluorocarbons, this is also a greenhouse gas. The lifetime of C_2F_6 in the atmosphere is 10 000 years and therefore has a high global warming potential.

Octafluorocyclobutane (*c*-C_4F_8) is also used in the plasma etching process. Since *c*-C_4F_8 can generate large quantities of CF_2 radicals due to electron impact on it, this is considered a very important gas with high etching sensitivity [7]. In addition to the semiconductor industry, Octafluorocyclobutane is used in retinal detachment surgery and as a gaseous dielectric, especially in gas mixtures. Due to its high lifetime in the atmosphere (3200 years), *c*-C_4F_8 this also considered as a global warming gas.

1.4. Experimental Techniques used to Measure the TCS

There are several methods used to measure the total electron scattering cross sections of atoms and molecules. Among those methods, the Ramsauer method and the linear transmission method are considered as the most successful and widely used methods. In addition to above mentioned techniques, some researches use the crossed beam technique, the time of flight technique or sometimes a combination of several techniques for cross section measurements.

In the Ramsauer method the electrons produced by a cathode (primarily a photo cathode) travel in a circular path inside the chamber. A uniform magnetic field, oriented

transverse to the plane of motion of the electron beam, is used for this purpose. The electron beam has to travel through several small slits before entering into the electron-gas scattering chamber which occupies the last 90º of the electron beam's trajectory. The purpose of the magnetic field is to enhance the angular resolution and for energy selection for both elastic and inelastic scattering. Those electrons that suffer inelastic collisions fail to pass through the slits; instead they move in a new circular path of smaller radius in the magnetic field. Figure 1.1 shows a schematic diagram of Ramsauer's apparatus [8].

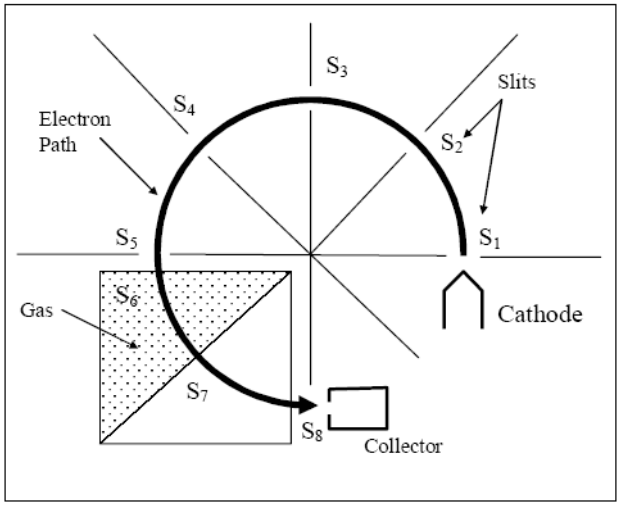

FIG. 1.1 A schematic diagram of the Ramsauer's apparatus.

During the experiment, current *j* to the collector, and *i* to the scattering chamber, were measured at various pressures. According to the Beer Lambert attenuation formula, *j* and *i* are related to the pressure *p* by;

$$j = (i+j) \exp [-\sigma lp] \qquad (1.3)$$

where l is the length of the path between slits S_6 and S_7 and σ is the total electron scattering cross section. In this method the coupling of energy selection and the scattering process together produce some experimental errors. As required by the experimental arrangement, both the applied voltage and magnetic field are changed for each energy. This leads to some uncertainty in systematic changes. Also, if the energy is obtained from a retarding potential measurement, the transverse magnetic field will introduce an uncertainty, whose energy has never been quantitatively analyzed [8].

The linear transmission technique, which was originally developed as a linearization of the Ramsauer method, is based on the measurement of the electron beam attenuation through a long gas cell. In this method the electron beam travels in a linear path and therefore eliminates the need of the magnetic field. When compared to the Ramsauer method, the linear transmission method produces more accurate results since there are no magnetic fields used as energy selectors. This will be discussed in detail under section 2.1. Also by employing one or more electrostatic analyzers as energy selectors the linear transmission technique can be improved to reduce the error caused by the forward-scattered electrons. Therefore the linear transmission technique with electro-static analyzers is considered as one of the most accurate technique used in total cross section measurements.

1.5. Previous Studies

Studies on electron interactions with fluorocarbon increased rapidly in the last decade or so mainly due to their applications in several important fields. In mid 1990's, the National Institute of Standards and Technology started a program to develop a database of electron collision cross sections and transport coefficients for plasma

processing gases relevant for the semiconductor industry. They also published several review articles [4, 5, 6, 7, 9, 10] about the present status and future needs during that period. Those publications emphasized the importance of fluorocarbon cross sections and data needed in that area. Therefore there is an increasing trend in fluorocarbon TCS studies, both experimental and theoretical, observed in the last ten to fifteen years' period.

1.5.1. CF_4 Total Cross Section Studies (in the Eenergy Range 0.10 – 4.50 keV)

The first reported TCS of CF_4 measurements were taken by Szmytkowski *et al*. [11] in 1992. This experiment was carried out using the linear transmission technique for the energy range 0.45 – 200 eV. Also in 1992, Zecca *et al*. [12] reported their TCS for CF_4 for the energy range 75 – 4000 eV. Zecca *et al*. used the Ramsauer technique for their measurements. In 1994, Sueoka *et al*. [13] published their results taken using the linear transmission technique. This experiment was carried out for the electrons with the energy ranging from 1 – 400 eV. In 2003, Ariyasinghe [14] reported CF_4 total cross sections in 100 – 1500 energy range. This is the first study on fluorocarbon cross sections carried out in this laboratory using the linear transmission technique. The most recent experimental TCS were reported by Manero *et al*. in 2002 [15] and then Nishimura et al. in 2003 [16]. Both of these groups used the linear transmission technique as their experimental method; Manero *et al*. carried out their work for 0.300 – 5.000 keV energy electrons while Nishimura *el al*. used 1.25 – 3000 eV energy electrons.

In 1992, Baluja *et al*. [17] reported the first theoretical total cross sections of CF_4, in the energy range 10 – 5000 eV. A parameter-free spherical complex optical potential (SCOP) approach is used for these calculations. In this method "the static, exchange,

polarization and absorption effects are determined from the electron density of the target by employing multicenter near Hartree-Fock wave functions" [17]. Unfortunately they didn't publish any of their calculated TCS but only gave a comparison graph with other published cross sections at that time. TCS calculated by Jiang et al. [18], for the energy range 10 – 1000 eV, were published in 1994. These calculations are based on the Additivity Rule and a model complex potential. The Adittivity Rule dates back to Bruche [19], ignores anisotropic electron-molecule interactions and the molecular problem is reduced to a much easier atomic problem. According to this method, the TCS of the target molecule is given by Equation 1.4. Here $Q_T(E)$ is the TCS of the molecule, at a given energy E, and $q^j_T(E)$ is the TCS due to the j^{th} atom of the molecule at the same energy.

$$Q_T(E) = \sum_{i=1}^{N} q_T^j(E) \tag{1.4}$$

The same approach, Additivity Rule with the complex optical potential method, is used by Jin-Feng *et al*. [20] for their calculations of CF_4 TCS. Their results were published in 2005 for the energy range of 100 – 5000 eV. Also in 2005, Antony *et al*. [21] presented their theoretical calculations for CF_4 TCS for 50 – 2000 eV energy electrons. A modified version of the Additivity Rule, termed as the Group Additivity Methhod by the author, is employed to calculate these cross sections. The Group Additivity Method is based on the use of TCS of each group in the target molecule to calculate the TCS of the molecule. For an example this method treats a X_2Y_4 molecule as the sum of two XY_2 groups and then uses (known) TCS of the XY_2 group to calculate the TCS for X_2Y_4.

1.5.2. CHF_3 Total Cross Section Studies (in the Energy Range 0.20 – 4.50 keV)

In 1998 Sueoka *et al*. [22] reported the first experimental TCS for CHF_3. This work was carried out using the linear transmission technique for the energy range 0.8 – 600 eV. At the same time period Iga and co-workers [23] conducted several experiments to measure the total cross section with differential and integral elastic cross sections of CHF_3. Although these results weren't published, they presented their findings at the International Symposium of Electron-Molecule Collisions and Swarms, in 1999. In 2005, Nishimura and Nakamura [24] also reported TCS for CHF_3 molecule, obtained by the linear transmission technique.

Semi-empirical values for CHF_3 TCS, calculated by Manero *et al*. [15], are published with their CF_4 TCS in 2002. For these calculations they used an empirical formula proposed Garcia and Manero [25], the same group, in 1997. According to this formula the TCS of a molecule is given by;

$$\sigma_T(E) = (0.4\,Z + 0.1\,\alpha + 0.7)\,E^{-0.78} \qquad (1.5)$$

where σ_T is the total scattering cross section in the units of Bohr radius square, Z is the number of target electrons, α is the polarizability of the target molecule in the units of Bohr radius cubed and E is the energy in keV. Although the validity of this formula is limited to molecules with 10 – 22 electrons, according to the original paper [25], the same formula is used in this work of Manero *et al*. [15] to calculate the TCS of CHF_3 which contains 34 electrons. Calculation of CHF_4 total cross sections by Jin-Feng *et al*. [20] was reported in 2005 with their CF_4 data. These calculations were performed using the same method discussed before, under the CF_4.

1.5.3. C_2F_6 Total Cross Section Studies (in the Energy Range 0.10 – 4.50 keV)

The first experimental TCS for C_2F_6 was reported by Szmytkowski *et al*. [26] in 2000. These TCS were measured using the linear transmission technique, for the energy range of 0.5 – 250 eV. In 2002, Sueoka *et al.* [27], also using the linear transmission technique, measured C_2F_6 cross sections for 0.8 – 600 eV energy electrons. In his 2003 work, Ariyasinghe [14] reported TCS for C_2F_6 for 100 – 1500 eV energy range. In the same year Nishimura *et al*. [16] also published their measurements for 1.25 – 3000 eV energy range.

Theoretical TCS for C_2F_6, calculated using the Additivity Rule (AR) and Energy-dependent Geometric Additivity Rule (EGAR), were published by Jiang et al [28] in 2000. These calculations were performed for 30 – 3000 eV energy electrons. The EGAR method is also based on the AR, but use the geometry of the molecule and the energy dependence of the TCS to make a more accurate calculation. According to this method, the TCS of a molecule $Q_{MT}(E)$ is given by;

$$Q_{MT}(E) = Q_{MG}(E) + A\,[Q_T(E) - Q_{MG}(E)] \qquad (1.6)$$

here, $Q_T(E)$ is the AR cross sections (given by Eq. 1.4), $Q_{MG}(E)$ is the geometric cross section and A is an energy dependent empirical correction factor for the particular molecule. The geometric cross section is calculated using the symmetry of the molecule and expressed by the following equation.

$$Q_{MG}(E) = \tfrac{1}{3}\, Q_{\parallel}(E) + \tfrac{2}{3}\, Q_{\perp}(E) \qquad (1.7)$$

Where $Q_{\parallel}(E)$ and $Q_{\perp}(E)$ are, respectively, the TCS for the electrons approaching the molecule parallel to the *Z*-axis and perpendicular to the *Z*-axis.

Anthony *et al*. [21] also reported their calculated TCS for C_2F_6 in 2005. Also in the same year Jin-Feng [20] published their TCS, based on the Additivity Rule, for C_2F_6. Both of these methods were discussed, in detailed, in section 1.5.1.

1.5.4. c-C_4F_8 Total Cross Section Studies (in the Energy Range 0.10 – 4.00 keV)

In 1999, Nishimura [29] presented the first reported total cross section measurements of *c*-C_4F_8, in the intermediate electron energy range, at the International Symposium on Electron-Molecule Collisions and Swarms. Although this work was not published, a more comprehensive study was done by the same group, Nishimura and Hamada [30], in 2007. This study was carried out using the linear transmission technique for 1 – 3000 eV energy electrons. In 2005, Makochekanwa *et al*. [31] reported their TCS for *c*-C_4F_8 for the energy reange 0.8 – 600 eV. This work was also performed using the linear transmission technique. Unfortunately there are no independent theoretical studies are reported in the literature on *c*-C_4F_8 TCS (in the intermediate energy range). The only available calculated TCS were reported by Christophorou and Olthoff [7] in their 2001 review paper titled Electron Interactions with *c*-C_4F_8. But here they use the available TCS to calculate their "suggested" TCS, using the least squares average of two sets in overlapping range and extending it to other energies.

1.5.5. C_3F_8 and C_4F_{10} Total Cross Section Studies (in the Energy Range 0.30 – 3.50 keV)

Since one of the objectives of the present experiment is to develop en empirical formula to predict TCS of linear fluorocarbons with single bonds, it is important to summarize past studies about C_3F_8 and C_4F_{10} gases although those TCS are not measured in this work. But TCS of those two gases, both experimental and theoretical, are important to test the validity of the proposed empirical formula.

In 1999 Tanaka *et al*. [32] published their C_3F_8 TCS for 0.8 – 600 eV energy range. This work was carried out using the linear transmission technique. Nishimura *et al*. [16] reported their measurements in 2003 with their (previously discussed) CF_4 and C_2F_6 measurements. There are two groups reporting theoretical C_3F_8 TCS and both those methods, Jiang *et al*. [28] and Anthony *et al*. [21], were discussed in previous sections.

The only published TCS (experimental or theoretical) for C_4F_{10} is reported by Makachekanwa *et al*. [33] in 2004. This study was performed using the linear transmission technique with 0.4 – 800 eV energy electrons.

1.6. The Proposed Experiment

As explained before, there is a huge demand for fluorocarbon cross sections due to its applications in several important fields. But so far there is very little work done in this area to develop an accurate data base on fluorocarbon total cross sections, especially at intermediate energy range. Some of the past works are limited to the low energy range while other works were carried out mainly in the high energy range. Also several reported TCS contain significant errors, mainly due to limitations in the experimental setups used to measure those TCS. For an example there are few groups mentioning the error caused by the forward scattering electrons since their setups are not equipped to overcome that problem.

The objective of this experiment is to measure the total electron scattering cross sections of several fluorocarbons, namely, CF_4 (Tetrafluoromethane), CHF_3 (Trifluoromethane), C_2F_6 (Hexafluoroethane), and *c*-C_4F_8 (Octafluorocyclobutane) for 0.10 – 4.50 keV energy electrons. To make a connection between the low energy data with intermediate energy data, the lower limit of the electron energy in this experiment is

set to 0.10 keV, which is common for most low energy studies. The measurements are taken using the linear transmission technique while electrostatic analyzers are used to increase the accuracy and overcome any affect caused by the forward scattering electrons. The results of this experiment are compared with the available experimental cross sections as well as the theoretical predictions. At the end a simple empirical formula is developed to predict the cross sections of linear fluorocarbons by analyzing the present measurements. The accuracy and the validity of the empirical formula are tested by comparing the predictions of the formula with present measurements and also with other experimental and theoretical cross sections available in the literature.

CHAPTER TWO

Experimental Method and Apparatus

2.1. Linear Transmission Technique

The attenuation of an electron beam, when travelling through a gas cell, is used as the principle of the linear transmission technique. In this technique currents of the primary electron beam and the attenuated electron beam, after passing through a gas cell of a known length, are being measured. The relationship between the primary and the attenuated beams can be expressed using the Lambert- Beer law as;

$$I = I_0 \exp(-NPL\sigma_T) \qquad (2.1)$$

where I is the attenuated electron beam current, I_0 is the primary electron beam current, N is the number density for unit pressure of target gas, P is the pressure inside the gas cell and L is the effective length of the cell. The total scattering cross section, σ_T, can be determined by using the slope of $ln\ (I/I_0)\ vs\ P$ graph. Figure 2.1 is a schematic diagram of the linear transmission technique.

FIG. 2.1. The linear transmission technique

The linear transmission technique is considered one of the simplest techniques available for total cross section measurements. But it is also considered as a technique

with a greater accuracy, when compared to other techniques where magnetic fields are used to track the electron beam [1]. As discussed by Blaauw *et a*l. [34] "it has been recognized that the use of a magnetic field as an energy selector, as in the Ramsauer technique, causes serious difficulties when one wants to calculate the influence of the spatial extent of the electron beam and of the electrons scattered into the solid angle of the detector on the measurement". With the use of electrostatic analyzers, the linear transmission technique can be used to measure only the attenuated electron beam, without being influenced by the scattered electrons or the secondary electrons.

2.2. Apparatus and Measurements

A schematic diagram of the experimental setup used for this experiment is given in Figure 2.2. A detailed description about this setup was given in several previous studies [35, 36, 37, 38]. Therefore only a brief description about the experimental setup is given below. New additions and methods used in this particular experiment are discussed in detail. Based on the functionality of different parts, the entire experiment arrangement system can be divided into three sub systems.

1. Electron production
2. Electron-gas interaction
3. Electron detection

2.2.1. Electron Production

The electron gun used in this experiment, Kimbal Physics EGG-3101, is capable of producing a well collimated, low current, small spot electron beam in the range 0.10 - 4.00 keV energy electrons. The EGG-3101 electron gun employs the thermionic emission to produce electrons with a pre-set energy. There is a refractory metal

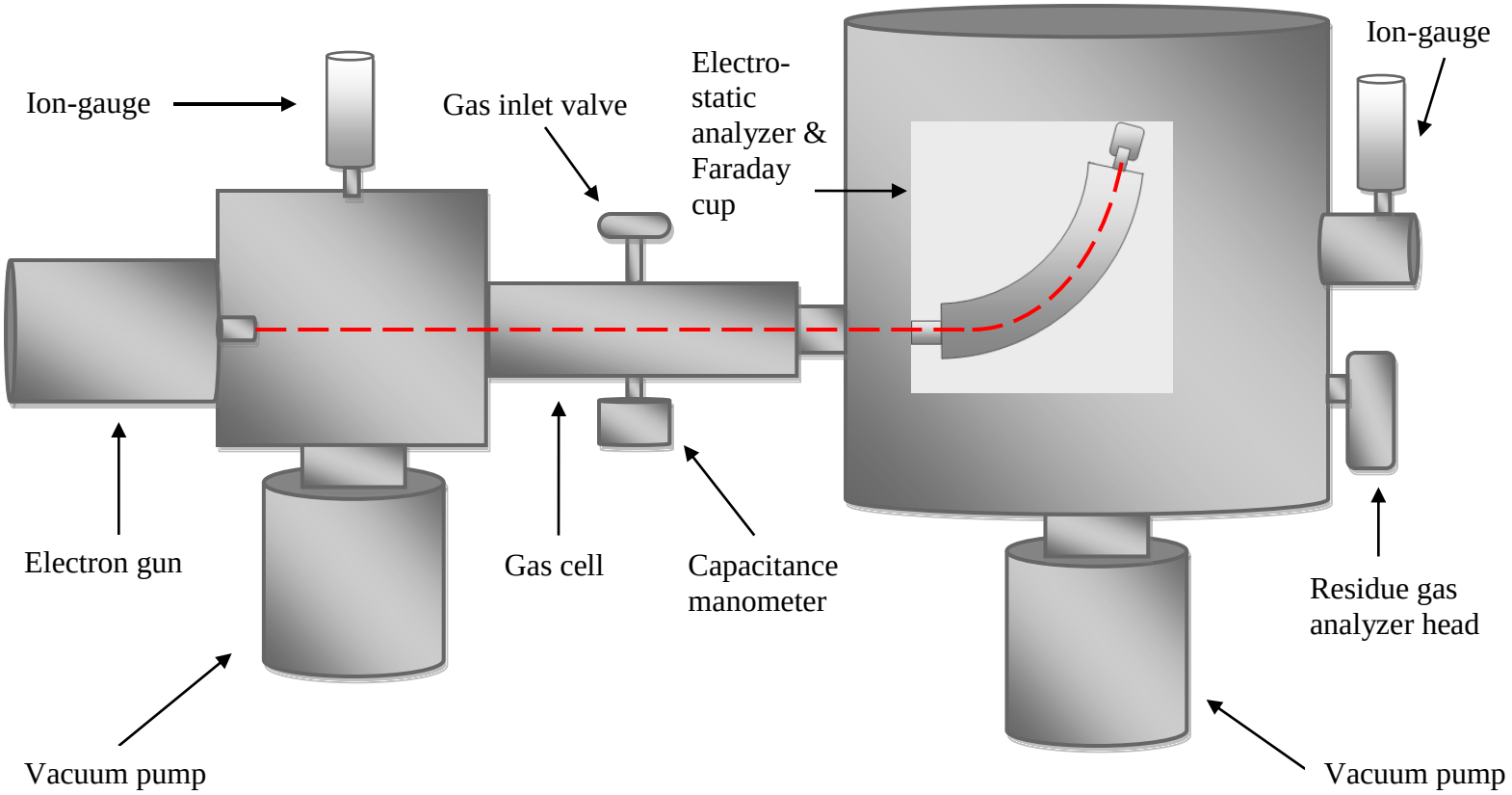

FIG. 2.2. The schematic diagram of the experimental setup

thermionic emitter consisting of a disk mounted on a hairpin filament [39]. This cathode starts to emit electrons when the filament wire is heated by a remote voltage source. The voltage source consists of an energy supply and a negative high voltage supply of 100 – 10000 V, reference to the ground. Three well-aligned 0.76 mm diameter apertures are used to collimate the electron beam emerging from electron gun. These apertures are fixed at the end of the electron gun 2 cm apart from each other.

In addition to the voltage source, EGG-3101 is equipped with a beam focusing device, a beam deflection mechanism, and a grid voltage controller to focus and control the electron beam. In this experiment, the grid voltage controller was used to adjust the electron beam current to a desired value. This is also recommended by the manufacturer [39]. Neither focusing nor deflection was used due to two reasons:

1. Throughout the experiment the primary electron beam current was kept at a constant value, 100 pA for electron energies higher than 0.80 keV and 200 pA for the lower electron energies. This was easily achieved by applying 20 μA or less filament emission current with the help of the grid voltage controller. Therefore the focus or the deflection was not required to control the electron beam.
2. It's been noticed that focus and/or deflection causes the electron beam to converge or diverge inside the gas cell. Converging or diverging the electron beam can not be used in transmission technique to obtain meaningful measurements of I_0 and I.

The electron gun is connected to a cylindrical vacuum chamber which is being pumped by a Leybold-Heraeus TURBOVAC 360SCV turbo-molecular pump to maintain the pressure at the electron gun area at 10^{-7} Torr or better. A Welch 1397 rough vacuum

pump is being used as the backing pump to support the TURBOVAC 360SCV. The pressure is continuously monitored by using an ion gauge and it wasn't allowed to exceed 10^{-6} Torr during the experiment. This precaution was taken to protect the filament of the electron gun, by preventing interactions between the filament and the target gas, so that emission properties of the filament remain the same throughout the experiment.

2.2.2. Electron-Gas Interaction

The electron beam leaving the electron gun enters into a cylindrical aluminum gas cell 24.5 cm long with the inside diameter of 2.54 cm. Inside the gas cell, energetic electrons interact with the target gas causing the electrons to scatter both elastically and inelastically. The entrance aperture and exit aperture of the gas cell, respectively, are 0.75 mm and 1.0 mm in diameter. The gas cell is shielded from the earth's and other stray magnetic fields using a μ-metal tube of 1.5 mm thickness. In the presence of this μ-metal shield, the magnetic field inside the gas cell measured to be in the milligauss region. A cross sectional view of the gas cell is given in Figure 2.3.

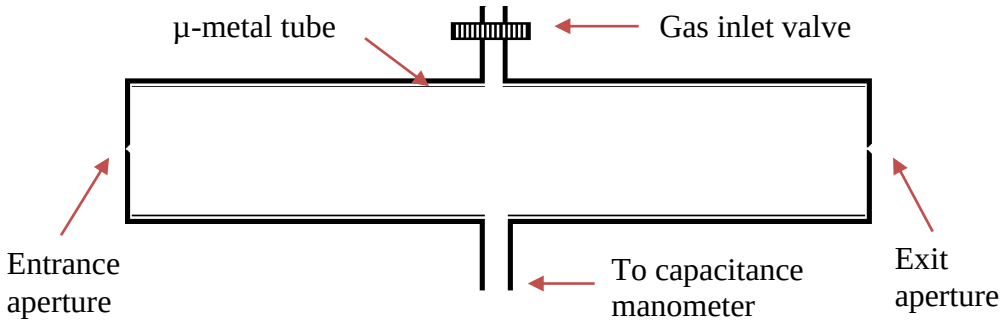

FIG. 2.3. A cross-sectional view of the gas cell

2.2.2.1. Measuring the Pressure inside the Gas Cell During most of the experiment a MKS Baratron 626A capacitance manometer was used to measure the gas pressure. This is mounted at the center of the gas cell. A MKS PDR-D digital readout

display unit is used to read the pressure measurement in the units of mTorr. The MKS Baratron 626A employs a sensor, consisting of a pressure inlet tube connected to a small chamber in transducer body, to record the pressure to the tenth place in mTorr. There is an elastic metal diaphragm, acting as a wall of the chamber, and the front panel of this diaphragm is exposed to the gas whose pressure is to be measured. The other side of the diaphragm faces to a ceramic disc with two electrodes. The bending of the diaphragm, as a response to the gas pressure, results in an imbalance in the electrode capacitances and that is converted into a dc voltage signal. Then this signal is sent through a signal conditioner to produce a precise signal and hence the pressure reading [40].

2.2.2.2. Calibration of the Capacitance Manometer using the Ion-Gauge While measuring cross sections at lower electron energies (< 0.30 keV) for C_4F_8, it was observed that the accuracy of the capacitance manometer was not sufficient due to the fact that even 0.4 mTorr pressure inside the gas cell was able to stop the electron beam completely. The cross section of C_4F_8 is relatively high at lower energies and therefore it was necessary to study the variation of the attenuated electron beam current for series of pressure values below 0.4 mTorr to determine the cross section at those energies. The readout unit of the capacitance manometer was not accurate enough to make pressure measurements below 0.1 mTorr or between 0.1 – 0.2 mTorr. Therefore the pressure measurements from the ion gauge attached to the scattering chamber, where the electrostatic analyzer is housed, was used to measure the pressure in the gas cell. First the variation of ion-gauge pressure, as a function of the gas cell pressure reading on the capacitance manometer, was studied for 0.0 – 5.0 mTorr range. From this study it was observed that the two pressure gauges vary linearly up to 0.5 mTorr gas cell pressure.

Figure 2.4 shows the variation of the ion-gauge pressure with the pressure reading on the capacitance manometer. During the experiment, with electron energy 0.40 keV and below, the ion-gauge pressure scale along with the calibration curve in Figure 2.4 is used to obtain the pressure in gas cell.

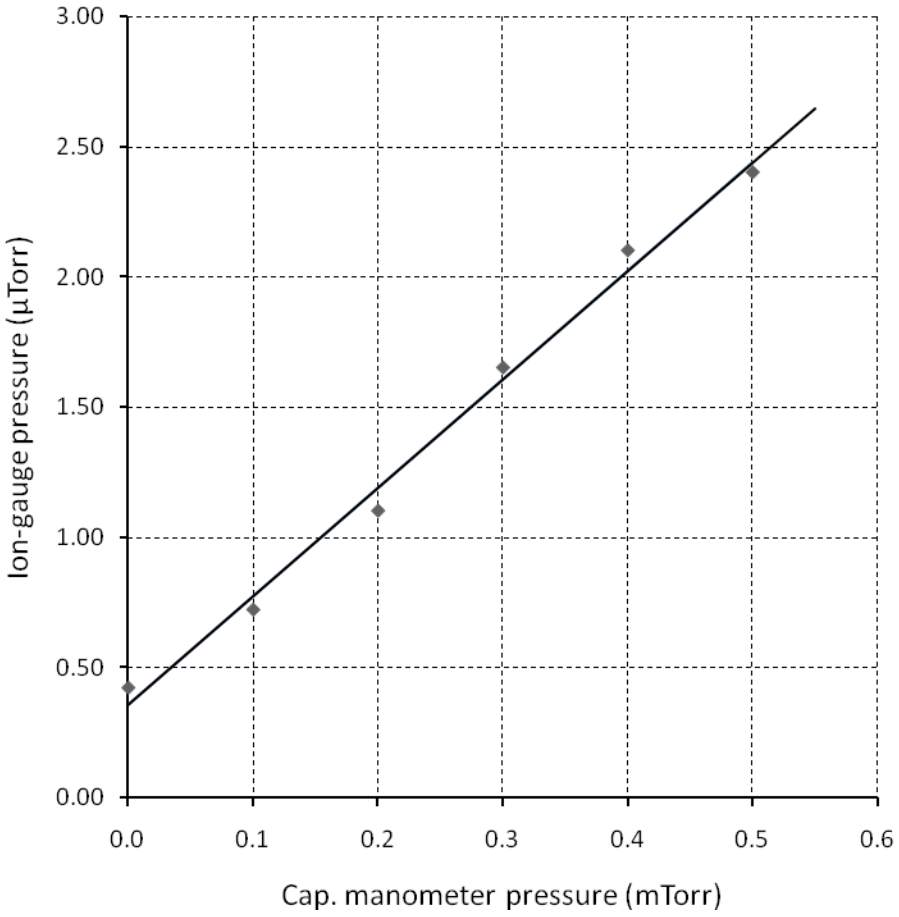

FIG. 2.4. The calibration curve for capacitance manometer

2.2.3. Electron Detection

A Comstock AC-902 double focusing electrostatic energy analyzer was used as the energy selector for the electron beam emerging from the gas-cell. A Faraday cup is mounted at the end of the electrostatic analyzer to collect the electrons with the required energy. This Faraday cup is connected to a Keithley 480 picoammeter to measure the

current of the electron beam in the units of pA. The electrostatic analyzer and the Faraday cup are housed inside a vacuum chamber made out of soft iron with an aluminum base plate. The vacuum chamber is pumped by a Leybold-Heraeus TURBOVAC 360SCV turbo-molecular pump which is mounted to the bottom of the chamber with a Welch 1397 rough pump as the backing pump. The pressure inside the chamber is measured by an ion-gauge and it's at low 10^{-7} Torr or better in the absence of the target gas. The pressure was at 10^{-6} Torr or better when the gas is present in the gas cell. To minimize the effect of the earth's and other magnetic fields, the chamber is shielded using a thick μ-metal layer. Also only the screws made out of non-magnetic alloys or stainless steel are used to connect parts of the vacuum chamber to avoid those being magnetized. Under these conditions the magnetic field inside the chamber is less than 10 milligauss.

Figure 2.5 shows a cross sectional view of the electro static analyzer-Faraday cup combination with circuit connections. The Comstock AC-902 electrostatic analyzer consists of two concentric 166° spherical sector surfaces, an inner convex surface of radius 48.8 mm and an outer concave surface of 60.7 mm, which are made from oxygen-free copper. The two surfaces are insulated from each other by using small sapphire balls between themselves and also between selectors and end plates. The side and end plates are held in position by non-magnetic stainless steel screws [41]. A retarding bias voltage, determined by the transmission voltage of electrons inside the electrostatic analyzer, is applied to the entrance and exit apertures of the analyzer by using BERTAN 230-03 high voltage power supplies. The bias voltage at a particular electron energy is calculated by subtracting the transmission voltage from the electron energy voltage. The transmission

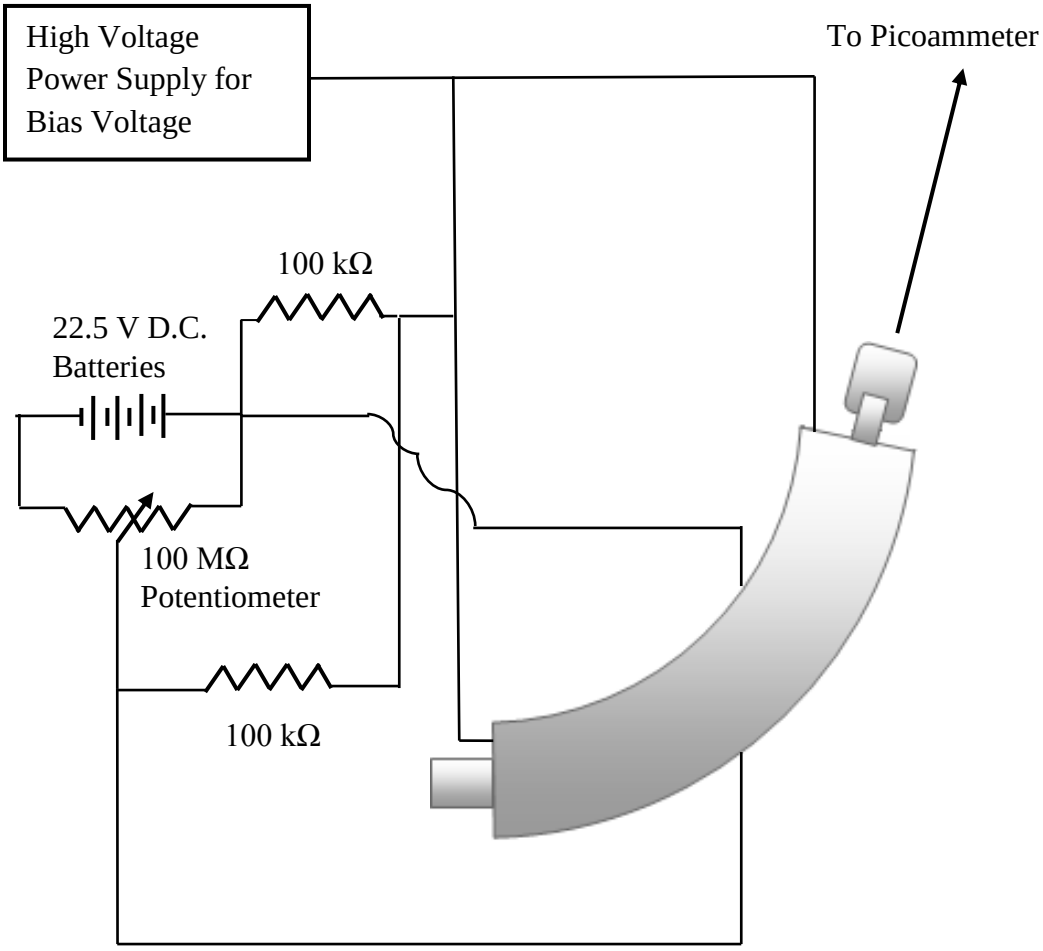

FIG. 2.5. Electrostatic analyzer and the Faraday cup circuit

voltage is set at 50 eV for 0.10 - 0.30 keV energy electrons, 100 eV for 0.40 - 1.80 keV energy electrons, and 150 eV for 2.00 - 4.00keV electrons. A potentiometer circuit was used to apply a constant voltage difference between two sectors of the electrostatic analyzer. The value of this voltage difference depends on the transmission voltage and it was 22.2 V for 50 eV transmissions, 44.4 V for 100 eV transmissions, and 66.6 V for 150eV transmissions. When these transmission voltages are applied to the electro static analyzer, only the electrons within the respective transmission energies are transmitted through the electrostatic analyzer and to the Faraday cup.

2.3. Experimental Procedure

Before starting the experiment, the purity of the gas cell was checked by using an Ametek Dycor 1200 quadrupole gas analyzer connected to the scattering chamber. This residue gas analyzer is capable of measuring the partial pressure of gases inside the chamber. Those partial pressures are displayed on a computer screen, in graphical or tabular forms, by using the Ametek Dycor model LC200 interface and software. Partial pressure of the target gas was checked against the partial pressure of N_2 and/or O_2, before and after admitting the gas into the gas cell. An additional Welch 1397 vacuum pump is used to purge the line till the required level of purity is obtained. During the experiment, the partial pressure of the target gas was always maintained at 99% or higher level.

After purging the gas delivery line and gas cell, the residue gas analyzer is used to verify that the partial pressure of the target gas is at the required level. The energy of the electron beam is set by the electron gun and the current of the un-attenuated beam is measured using the picoammeter. Then the primary beam current is set to a constant value at 100 pA (200 pA for lower energies) using the electron gun's source current controller and the grid voltage controller. After allowing enough time (about 30 minutes) for the electron gun to warm up and electron beam to settle down at the required energy, the inlet valve of the gas cell is opened slowly to let the target gas enters into the gas cell. The beam current of the attenuated electron beam is recorded with the pressure inside the gas cell. Then the valve is closed and a sufficient time (about 4-5 minutes) is given to the system to pump down and return to the initial pressure. About 8-9 data readings, at different pressures, are taken at each trial. The gas cell pressure is always kept below 4.0 mTorr to prevent the electron gun filament being exposed to the target gas. For each

electron beam energy, 6-8 similar trials are performed before calculating the average cross section for the particular energy. To obtain the cross section at a different energy, the electron beam energy is changed to the new value and then the same procedure is repeated at that energy.

The temperature near the gas cell is measured during the experiment using a mercury-glass thermometer. Since any temperature variation could affect the number density of the target gas, the temperature controller of the lab is set to a constant value throughout the experiment.

2.4. Accuracy of Measurements and Experimental Errors

There are three main parameters, electron energy, gas cell pressure and electron beam current, associated with this experiment and those are measured in each trial. Other parameters such as length of the gas cell, temperature, purity of the gas, are kept as constants throughout the experiment. Accuracy of each measurement is determined by the measuring instrument used to make that measurement. The final error of the total scattering cross section is calculated by using the squares of each error and applying the standard propagation error technique.

The energy of the electron beam is recorded from the display unit of the electron gun which has an accuracy of 0.01 keV. This error is higher than the energy spread error of the electron beam, ± 0.4 eV [39]. The readout error of ± 0.01 keV remains a constant for all the energies studied in this experiment.

The current of the primary electron beam is set at 100 pA (200 pA for lower energies) constant value for this experiment with an error of ± 1 pA. Since the stability of the electron beam is reduced with time (± 0.1% per hour [39]), fluctuations in the

electron current are observed after running the experiment for several hours. To minimize this error, the maximum continuous running time of the experiment is limited to 6 hours. After considering all these facts, the contribution of the current error to the total cross section is estimated to be 1% or less.

As discussed in 2.2.2.1, the pressure inside the gas cell is measured using the capacitance manometer for electron energies higher than 0.30 keV. The accuracy of the capacitance manometer is limited to 0.1 mTorr. When the ion-gauge calibration method is used to measure the pressure, for electron energies < 0.30 keV, the accuracy of pressure measurement increased to 0.01 mTorr. The estimated error to the total cross section from pressure measurement is taken as 2% or less.

Although the geometric length of the gas cell used in this experiment is 24.5 cm, the effective electron-gas interaction length is different from that due to effusion of gas molecules through entrance and exit apertures. This effect has been studied in detail in a previous work [42] and according to that study the effective length is ±3 mm off, for each side, from the geometric length. Therefore the final length error is calculated as 2.5%.

All the gases used in this experiment were purchased from the Matheson Tri-Gas, Inc. within minimum purity of 99.9% or better. Also, before the experiment the gas line and gas cell are purged to confirm, by the RGA, that 99% or more target gas is present inside the gas cell. Since all the gases studied in this experiment can be considered as heavy gases (molecular mass is higher than that of N_2), it is estimated that the error contribution to the total cross section is 1% or less.

The temperature near the gas cell remains as a constant, 22°C, during the experiment. In two previous studies, it was observed that there is no significant

temperature difference between the inside and immediate outside of the gas cell [37]. Therefore the number density (N) of the target gas remains a constant throughout the experiment and there is no error contribution, from the temperature, to the total cross section.

After considering all the above facts, the final error for the total scattering cross section is estimated as ±4% or less for CF_4 and CHF_3 gases. It came out to be ±5% or less for C_2F_6 and *c*-C_4F_8 gases.

CHAPTER THREE

Results and Analysis

3.1. Calculation of the Total Electron Scattering Cross Section

As explained in Chapter Two, the total electron scattering cross section (σ_T), at a given energy, can be calculated by using measured values of attenuated current (*I*), pressure inside the gas cell (*P*), gas cell length (*L*) and the number density (*N*). By rearranging the variables, Eq. 2.1 can be expressed as;

$$\sigma_T = \left| \text{Slope} \right| / \text{NL} \qquad (3.1)$$

here $\left| \text{Slope} \right|$ is the absolute value of the slope of the best fit line (linear regression line) of *ln* (I/I_0) *vs P* graph. For a given energy there were 6 - 8 independent trials and only those with square of the correlation coefficient (R^2) > 99% were selected for TCS calculations. Also more than 95% of the trials in this experiment produced best fit lines with $R^2 > 99$ % or better. Figure 3.1 shows the graph of ln (I/I_0) vs Pressure, obtained for various electron energies, for CF_4. Similar plots for CHF_3, C_2F_6 and *c*-C_4F_8, respectively, are presented in Figures 3.2, 3.3 and 3.4.

The total electron scattering cross section is obtained by dividing the $\left| \text{Slope} \right|$ by the length of the gas cell, which is 24.5 cm for this experiment, and the number density of the target gas at 22°C. As explained in the Chapter Two, the combined error of this calculation, after including all the experimental errors, came out to be ±4% or less for CF_4 and CHF_3 gases while it's ±5% or less for C_2F_6 and *c*-C_4F_8 gases. The measured total electron scattering cross sections for CF_4 and CHF_3 are summarized in Table 3.1

with associated errors. Table 3.2 gives a summary of C_2F_6 and *c*-C_4F_8 total cross sections with corresponding errors.

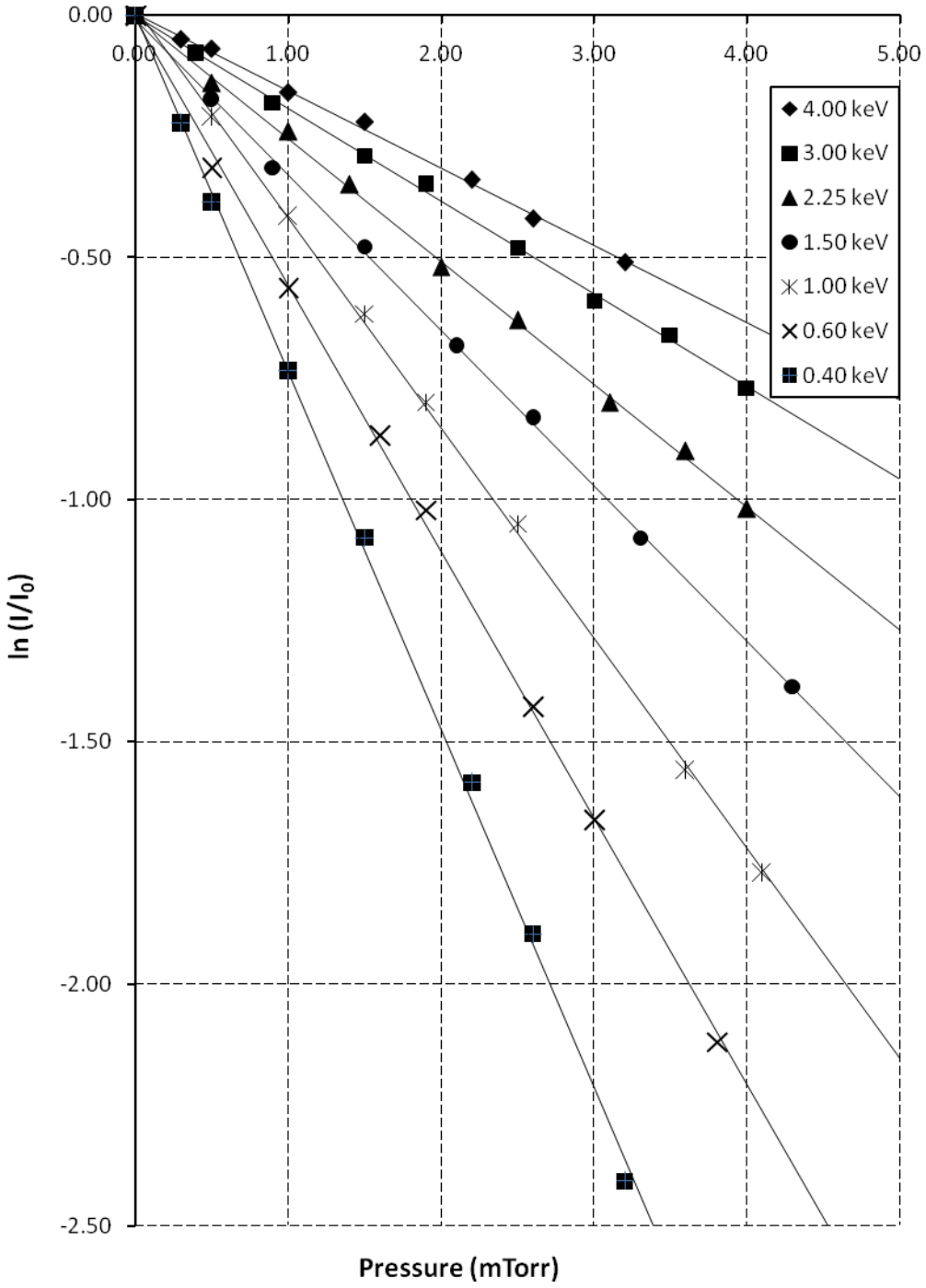

FIG. 3.1. The graph of ln (I/I_0) vs Pressure for CF_4 at various electron energies.

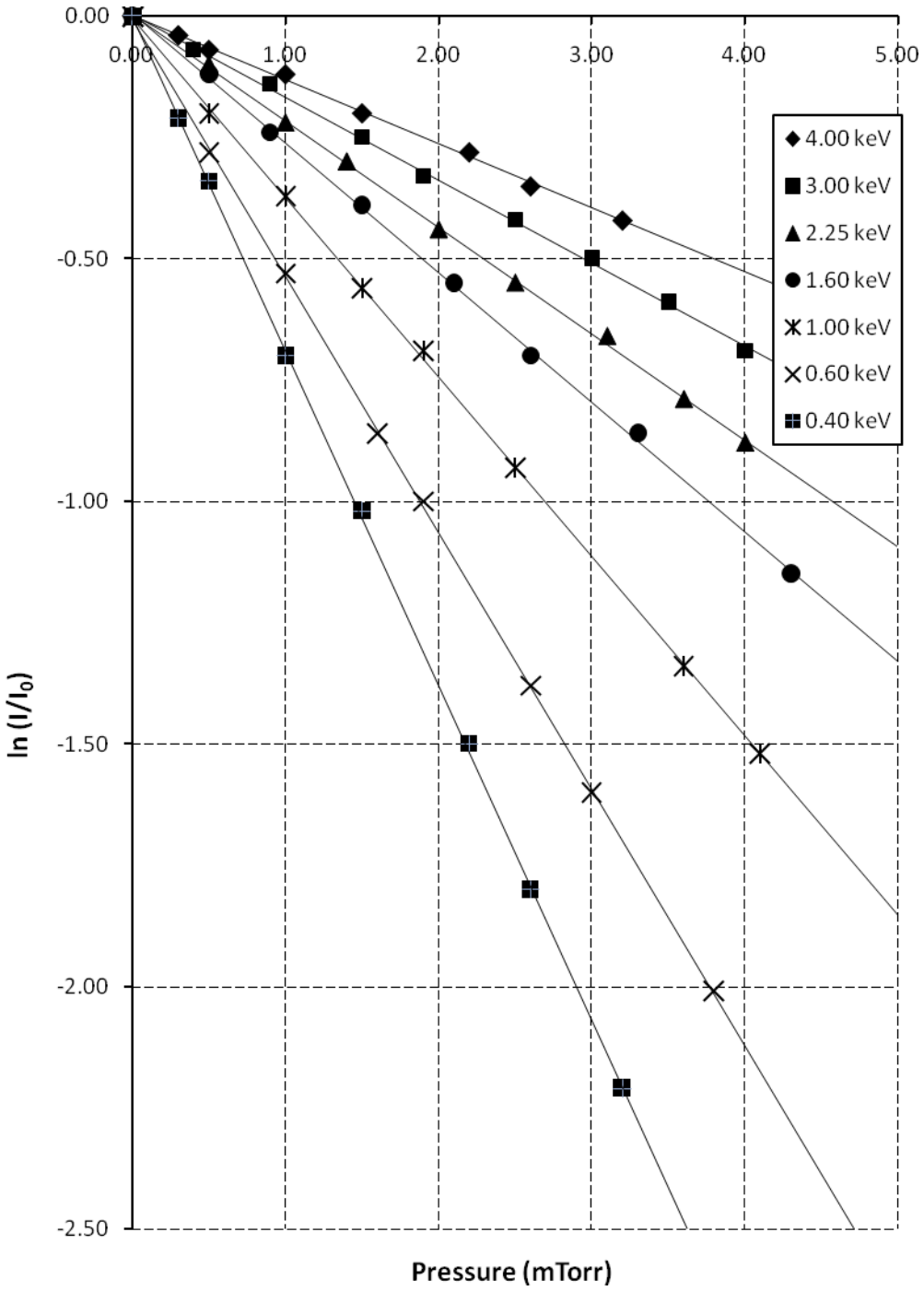

FIG. 3.2. The graph of ln (I/I_0) vs Pressure for CHF_3 at various electron energies.

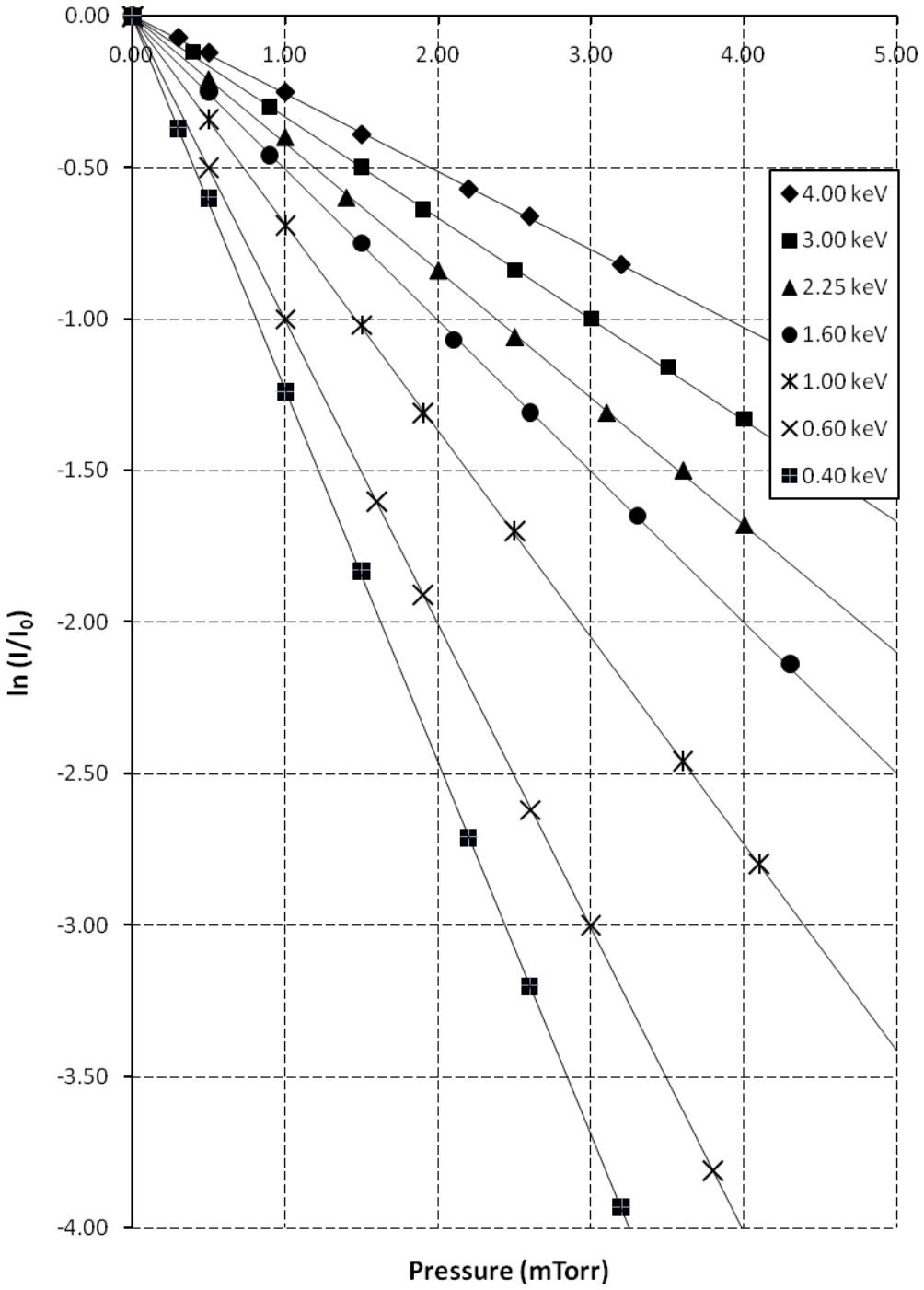

FIG. 3.3. The graph of ln (I/I_0) vs Pressure for C_2F_6 at various electron energies.

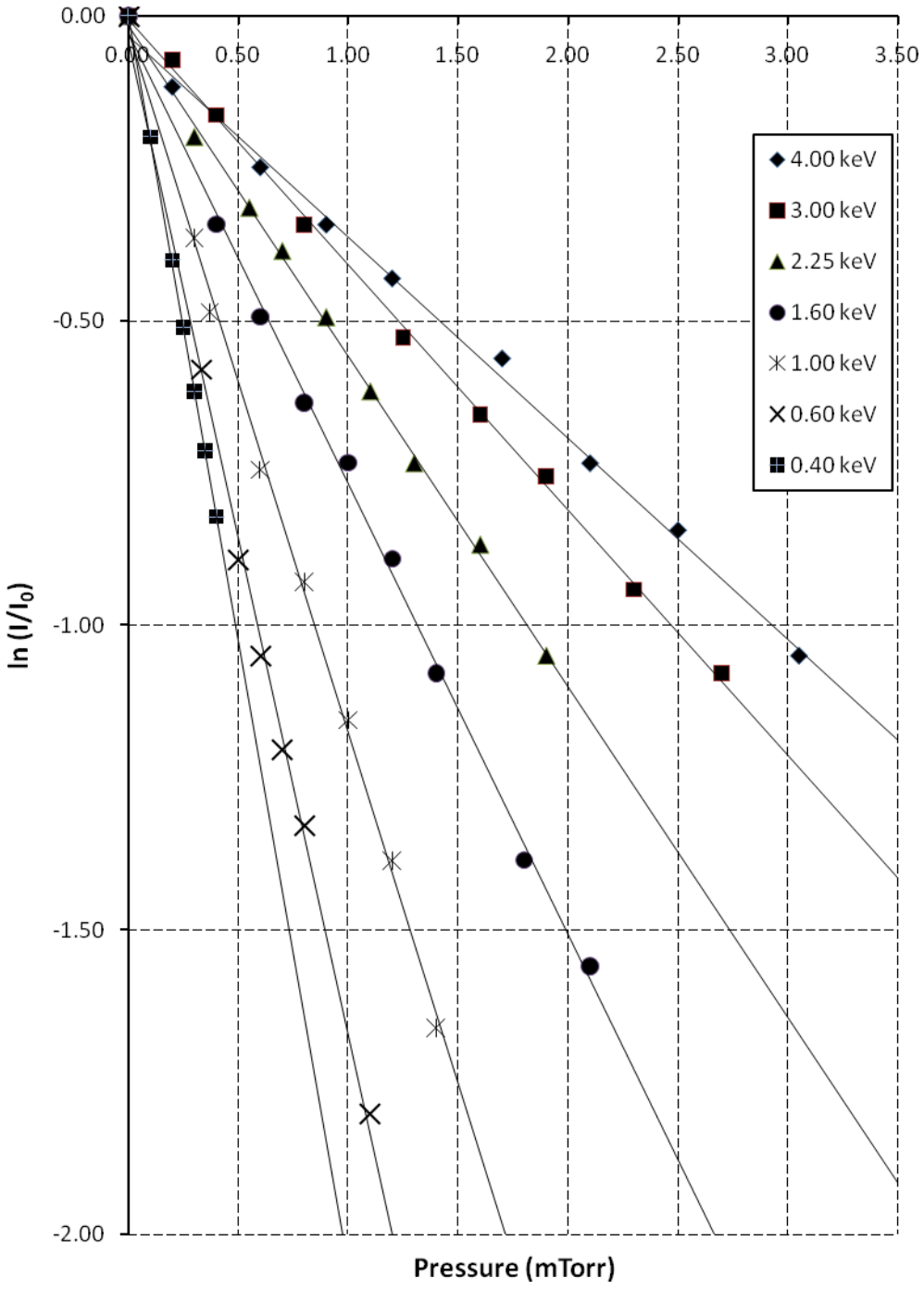

FIG 3.4. The graph of ln (I/I_0) vs Pressure for c-C_4F_8 at various electron energies.

TABLE 3.1. Measured total electron scattering cross sections of CF_4 and CHF_3 in units of 10^{-20} m^2

Energy (keV)	CF_4	CHF_3
0.100	18.4 ± 0.7	
0.20	13.6 ± 0.6	11.6 ± 0.5
0.30	10.8 ± 0.4	9.28 ± 0.37
0.40	9.44 ± 0.38	8.01 ± 0.32
0.50	8.53 ± 0.34	7.11 ± 0.28
0.60	7.28 ± 0.29	6.16 ± 0.25
0.70	6.48 ± 0.26	5.47 ± 0.22
0.80	5.98 ± 0.24	5.05 ± 0.20
0.90	5.51 ± 0.22	4.61 ± 0.18
1.00	5.21 ± 0.21	4.13 ± 0.17
1.10	4.70 ± 0.19	3.92 ± 0.16
1.20	4.35 ± 0.17	3.65 ± 0.15
1.40	3.90 ± 0.16	3.26 ± 0.13
1.50	3.79 ± 0.15	
1.60	3.65 ± 0.15	3.07 ± 0.12
1.80	3.40 ± 0.14	2.87 ± 0.11
2.00	3.22 ± 0.13	2.66 ± 0.11
2.25	2.95 ± 0.12	2.53 ± 0.10
2.50	2.62 ± 0.10	2.34 ± 0.09
2.75	2.51 ± 0.10	2.15 ± 0.09
3.00	2.20 ± 0.09	1.97 ± 0.08
3.50	2.01 ± 0.08	1.73 ± 0.07
4.00	1.81 ± 0.07	1.50 ± 0.06
4.50	1.60 ± 0.06	1.35 ± 0.05

TABLE 3.2. Measured total electron scattering cross sections of C_2F_6 and C_4F_8 in units of 10^{-20} m^2

Energy (keV)	C_2F_6	C_4F_8
0.100	28.2 ± 1.4	
0.125		43.3 ± 2.2
0.150		40.3 ± 2.0
0.20	19.9 ± 1.0	37.3 ± 1.9
0.25		32.1 ± 1.6
0.30	16.9 ± 0.8	27.8 ± 1.4
0.40	14.3 ± 0.7	25.2 ± 1.3
0.50	12.7 ± 0.6	21.8 ± 1.1
0.60	11.6 ± 0.6	19.7 ± 1.0
0.70	10.2 ± 0.5	17.7 ± 0.9
0.80	9.47 ± 0.47	15.9 ± 0.8
0.90	8.62 ± 0.43	14.7 ± 0.7
1.00	7.92 ± 0.40	13.7 ± 0.7
1.10	7.60 ± 0.38	
1.20	7.19 ± 0.36	11.6 ± 0.6
1.40	6.39 ± 0.32	10.2 ± 0.5
1.60	5.79 ± 0.29	9.17 ± 0.46
1.80	5.36 ± 0.27	8.22 ± 0.41
2.00	5.09 ± 0.25	7.75 ± 0.39
2.25	4.87 ± 0.24	6.87 ± 0.34
2.50	4.47 ± 0.22	6.22 ± 0.31
2.75	4.18 ± 0.21	5.60 ± 0.28
3.00	3.84 ± 0.19	5.15 ± 0.26
3.50	3.42 ± 0.17	4.66 ± 0.23
4.00	2.94 ± 0.15	4.20 ± 0.21
4.50	2.59 ± 0.13	

3.2. Comparison of Measured Total Cross Sections with Those in Literature

As discussed in Chapter One, in the last ten years or so there was a greater interest in electron-molecule interactions of plasma processing gases mainly due to their importance and applications. But most of those studies were carried out with low energy electrons. Not only very few experimental and theoretical TCS are available for the intermediate energy range (~ 0.40 – 4.00 keV), but also there are significant disagreements between those TCS, too. In this chapter, the total electron scattering cross sections measured in this experiment are compared to existing experimental and theoretical cross sections in the literature.

3.2.1. Tetrafluoromethane (CF_4)

Among the gases studied in this experiment, CF_4 is the most studied gas by other research groups and therefore sufficient TCS data, both experimental and theoretical, is available for a comparison.

There are five reported experimental works on CF_4 TCS measurements with overlapping electron energies as in the present experiment. Those TCS are compared with the TCS produced in this experiment in Figure 3.5. In the same figure, available theoretical TCS of CF_4 are also presented as a function of electron energy. Since all data points are somewhat clumped together, all the available total cross sections are presented in Table 3.3 to study the deviation between TCS reported by different groups.

Out of the experimental groups, total cross sections measured by Zecca *et al*. [12] and Manero *et al*. [15] are in very good agreement with the present measurements (less than 5% difference) below 2.00 keV electron energy. At 2.00 keV and higher energies, TCS produced by Zecca *et al*. are 7 - 20 % lower than the present measurements and

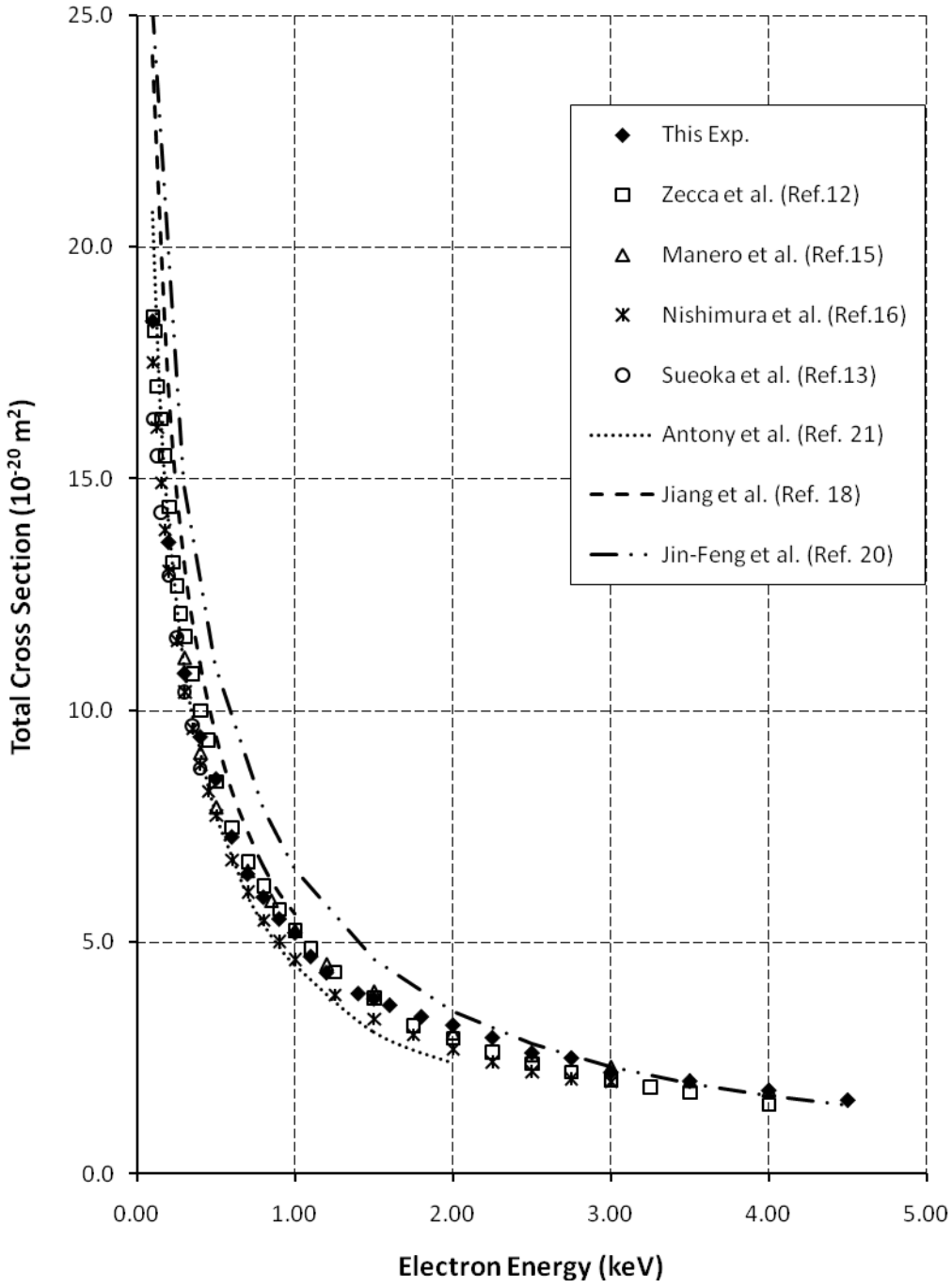

FIG. 3.5. A comparison of present CF_4 TCS with those produced by other experimental and theoretical groups. Dashed lines represent theoretical TCS.

TABLE 3.3. The summary of experimental and theoretical total electron scattering cross section of CF_4 in units of 10^{-20} m^2.

	Experimental TCS				Theoretical TCS			
Energy (keV)	This Exp.	Zecca [12]	Manero [15]	Nishim-ura [16]	Sueoka [13]	Antony [21]	Jiang [18]	Jin-Feng [20]
0.100	18.41	18.5		17.5	16.28	20.76	24.14	25.18
0.110		18.2						
0.120					15.49			
0.125		17.0		16.1				
0.150		16.3		14.9	14.27	16.54		
0.175		15.5		13.9				
0.200	13.64	14.4		13.0	12.91	14.12	17.02	
0.225		13.2						
0.250		12.7		11.5	11.57			
0.275		12.1						
0.300	10.81	11.6	11.14	10.4	10.40	10.94	13.21	14.89
0.350		10.8		9.6	9.68			
0.40	9.44	10.0	9.09	8.83	8.76	9.16	11.04	
0.45		9.37		8.26				
0.50	8.53	8.47	7.91	7.74		7.77	9.48	10.98
0.60	7.28	7.48		6.77		6.88	8.29	
0.70	6.48	6.74	6.54	6.09		6.01	7.41	
0.80	5.98	6.22		5.48		5.40	6.65	7.87
0.85			5.89					
0.90	5.51	5.71		5.02		4.91	6.07	
1.00	5.21	5.26	5.25	4.63		4.51	5.62	6.59
1.10	4.70	4.87						
1.20	4.35		4.52					
1.25		4.37		3.87				
1.40	3.90							
1.50	3.79	3.81	3.93	3.35		3.06		4.62
1.60	3.65							
1.75		3.21		3.01				
1.80	3.40							
2.00	3.22	2.94	3.03	2.69		2.39		3.51
2.25	2.95	2.64		2.42				
2.50	2.62	2.39	2.56	2.22				2.80
2.75	2.51	2.21		2.06				
3.00	2.20	2.03	2.30	2.00				2.31
3.25		1.88						
3.50	2.01	1.77	2.00					1.96
4.00	1.81	1.51	1.80					1.69
4.50	1.60							1.48

those reported by Manero *et al*. It is important to state that both the present TCS and TCS reported by Manero *et al*. are based on the linear transmission technique while those of Zecca *et al*. are based on the Ramsauer technique. TCS measured by both Nishimura *et al*. [16] and Sueoka *et al*. [13] are very close to each other and 5 - 15% lower than TCS obtained in this experiment. According to references [13] and [16], both these groups had to make corrections to their measured cross sections, to compensate for the electrons scattered in the forward direction. It's interesting to notice that this correction came out to be, at some energies, about 14% of their measured total cross section. As explained in Chapters One and Two, measurements taken in this laboratory are barely influenced by the electron scattered in the forward direction due to the experimental technique employed. Therefore it is reasonable to expect that TCS reported by Nishimura *et al*. [16] and Sueoka *et al*. [13] are lower than those measured in this experiment. Although Szmytkowski *et al*. [11] also reported their experimental results for CF_4, it is difficult to make any meaningful comparison with that data due to the narrow overlapping energy range between the two works. Only the TCS measurements made at 0.10 keV and 0.20 keV are common for both studies.

There are three sets of calculated TCS of CF_4 are available in the literature. Predictions made by Antony *et al*. [21] are in good agreement (less than 10% difference) with TCS measured in this lab and also with measurements taken in other labs. Calculated TCS by Jiang *et al*. [18] are higher than (8 - 25 %) than present measurements and also higher than TCS reported by other experimental groups. Although it seems like TCS by Jiang *et al*. and this work tend to agree with each other with the increasing electron energy, it's difficult to draw a conclusion from that because the comparison is

only possible up to 1.00 keV. There are no reported total cross sections by Jiang *et al*. [18] above 1.00 keV. TCS predicted by Jin-Feng *et al*. [20] are about 45% higher than present measurements at lower electron energies. But with the increasing energy the difference becomes smaller and both TCS are in good agreement at higher (above 2.50 keV) electron energies.

3.2.2. Trifluoromethane (CHF_3)

Experimental TCS of trifluoromethane produced by different experimental and theoretical groups are compared in Figure 3.6. Also those TCS are presented in tabular form in the Table 3.4 to study the deviation between different measurements.

When compared with experimental CHF_3 cross sections reported in literature, measurements made by Iga *et al*. [23] are in very good agreement, within experimental uncertainties, with TCS measured in the present experiment. The difference between total cross sections measured by Nishimura and Nakamura [24] and those measured in the present study is relatively low (5 %) at lower energies up to 1.00 keV. With the increasing electron energy the difference between two measurements gets wider, about 10% difference, with present measurements being higher. As discussed before, under CF_4 analysis, there is a correction made by Nishimura and Nakamura for the forward scattering electrons. The difference between the present TCS and those produced by Nishimura and Nakamura could be due to under-correction for the forward-scattered electrons. A comparison between Sueoka *et al*. [22] and present work is only possible in the 0.20 – 0.60 keV range. Within that energy range, the observed difference between two studies is less than 10 % with present measurements always higher. Since the

experimental setup used by Sueoka *et al*. is also subjected to the forward scattering electrons, this difference could easily be explained.

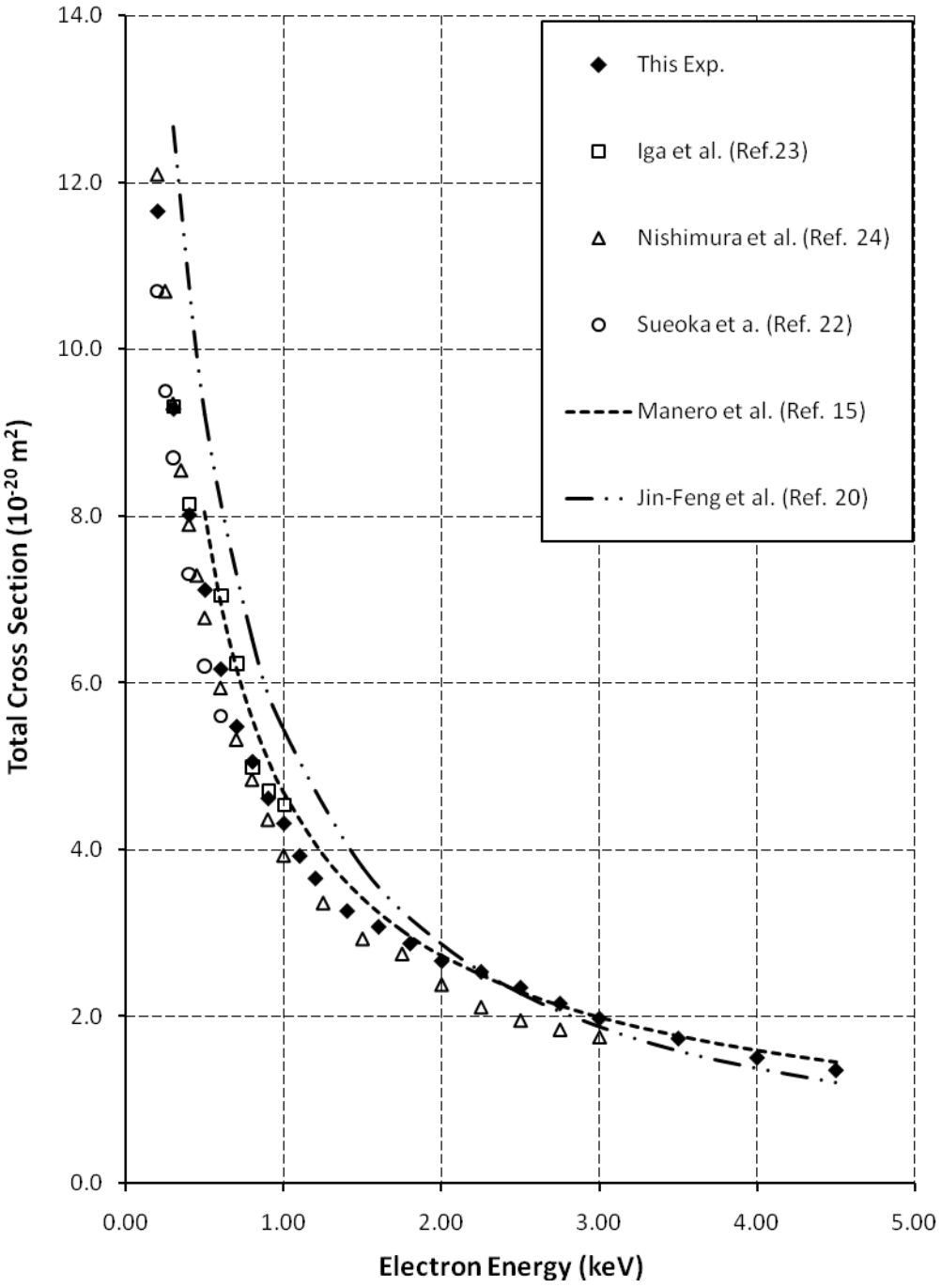

FIG. 3.6. A comparison of present CHF_3 TCS with those produced by other experimental and theoretical groups. Dashed lines represent theoretical TCS.

TABLE 3.4. The summary of experimental and theoretical/empirical total electron scattering cross section of CHF_3 in units of 10^{-20} m^2.

	Experimental TCS				Theoretical TCS	
Energy	This	Iga	Nishimura	Sueoka	Manero	Jin-Feng
(keV)	Exp.	[23]	[24]	[22]	[15]	[20]
0.200	11.65		12.1	10.7		
0.25			10.7	9.5		
0.30	9.28	9.30	9.35	8.7		12.66
0.35			8.55			
0.40	8.01	8.14	7.90	7.3		
0.45			7.29			
0.50	7.11		6.78	6.2	8.05	9.21
0.60	6.16	7.04	5.94	5.6	6.99	
0.70	5.47	6.23	5.32		6.19	
0.80	5.05	4.98	4.84		5.58	6.52
0.90	4.61	4.69	4.36		5.09	
1.00	4.31	4.53	3.93		4.69	5.43
1.10	3.92					
1.20	3.65					
1.25			3.36		3.94	
1.30						
1.40	3.26					
1.50			2.93		3.42	3.78
1.60	3.07					
1.75			2.75		3.03	
1.80	2.87					
2.00	2.66		2.38		2.73	2.86
2.25	2.53		2.11			
2.50	2.34		1.95		2.30	2.27
2.75	2.15		1.84			
3.00	1.97		1.75		1.99	1.87
3.50	1.73				1.77	1.58
4.00	1.5				1.59	1.37
4.50	1.35				1.45	1.20

The calculated total scattering cross sections by Manero *et al*. [15], using their empirical formula – Eq. 1.5, slightly higher than TCS measured in this study. The greatest difference is observed at the lowest energy (13 %) and the difference decreases with the increasing electron energy. Although this empirical formula is developed to predict TCS for molecules with 10-22 electrons [25], it is interesting to see that they used it to calculate TCS of CHF_3, which consists 34 electrons. The only theoretical calculations of CHF_3 cross sections were reported by Jin-Feng *et al*. [20]. As in CF_4, their calculations are about 35% higher than present measurements at lower electron energies. But with the increasing electron energy the difference becomes smaller (about 3 - 5 %) and both TCS agree with each other at higher energies.

3.2.3. Hexafluoroethane (C_2F_6)

A comparison of C_2F_6 TCS, reported by different experimental and theoretical groups, is presented in Figure 3.7. A summary of those TCS is given in Table 3.5 to study the deviation between them.

Among experimental TCS of C_2F_6 reported in the literature, those of Szmytkowski *et at*. [26] are in very good agreement with present measurements, within experimental uncertainties, at lower energies. A comparison is not possible at higher electron energies since Szmytkowski *et al*. only report total cross sections up to 0.25 keV. TCS reported by Nishimura *et al*. [16] are 3 - 13 % different from those measured in this lab. Also present measurements are slightly higher than those of Nishimura *et al*. This could be due the fact that their experiment is affected by forward scattering electrons and hence TCS measurements are lower than the correct results. Although they had made a correction to compensate for that effect, it's noticed that all TCS reported by

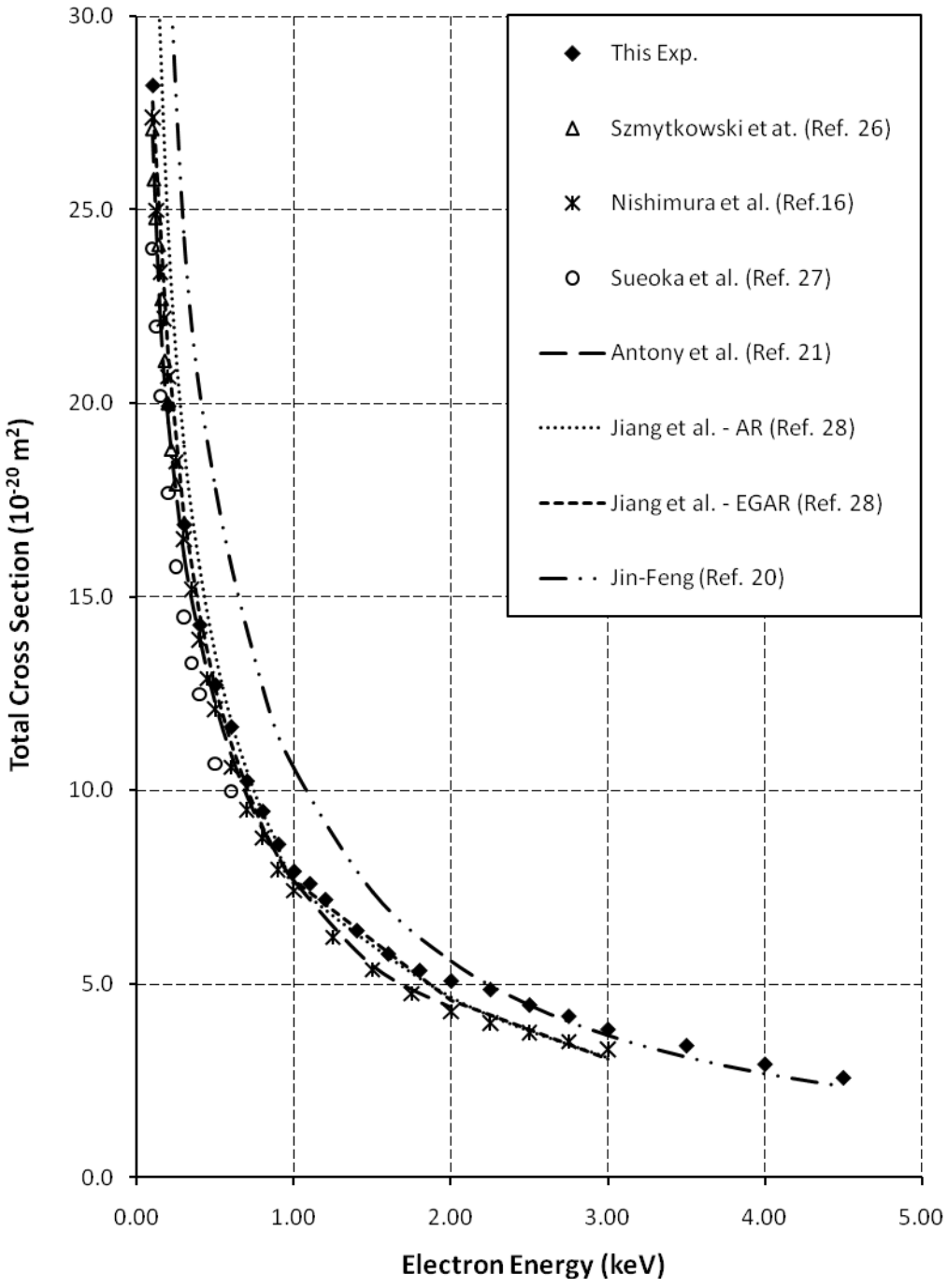

FIG. 3.7. A comparison of present C_2F_6 TCS with those produced by other experimental and theoretical groups. Dashed lines represent theoretical TCS.

TABLE 3.5. The summary of experimental and theoretical total electron scattering cross section of C_2F_6 in units of 10^{-20} m^2.

	Experimental TCS					Theoretical TCS		
Energy (keV)	This Exp.	Szmytko-wski [26]	Nishim-ura [16]	Sueoka [27]	Antony [21]	Jiang (AR) [28]	Jiang (EGAR) [128]	Jin-Feng [20]
0.100	28.21	27.1	27.4	24.0	26.90	34.75	27.80	41.32
0.110		25.8						
0.120		24.8						
0.125			25.0	22.0				
0.140		24.1						
0.150			23.4	20.2	22.15			
0.160		22.7						
0.180		21.1	22.2					
0.200	19.93	20.0	20.7	17.7	19.51	24.39	21.23	
0.22		18.8						
0.25		17.9	18.5	15.8				
0.30	16.87		16.5	14.5	16.07	18.91	17.10	24.29
0.35			15.2	13.3				
0.40	14.28		13.9	12.5	13.94	15.76	14.56	
0.45			12.9					
0.50	12.73		12.1	10.7	12.24	13.51	12.65	17.80
0.60	11.65		10.6	10.0	10.93	11.80	11.16	
0.70	10.25		9.50		9.87	10.52	10.02	
0.80	9.47		8.78		9.00	9.43	9.03	12.67
0.90	8.62		7.96		8.28	8.59	8.26	
1.00	7.92		7.42		7.67	7.59	7.68	10.58
1.10	7.6							
1.20	7.19							
1.25			6.21					
1.40	6.39							
1.50			5.38		5.48			7.39
1.60	5.79							
1.75			4.76					
1.80	5.36							
2.00	5.09		4.30		4.40	4.66	4.57	5.60
2.25	4.87		4.00					
2.50	4.47		3.75					4.46
2.75	4.18		3.52					
3.00	3.84		3.31			3.09	3.05	3.68
3.50	3.42							3.12
4.00	2.94							2.69
4.50	2.59							2.36

Nishimura *et al*. [3, 10, 17], for CF_4, CHF_3 and C_2F_6, are lower than those measured in this lab and other labs. Similarly TCS reported by Sueoka *et al*. [27], also influenced by forward scattering electrons, are lower than TCS measured in this lab by 10 - 15 %.

Among theoretical TCS, calculations made by Antony *et al.* [21] are in good agreement with current measurements in 0.10 – 1.00 keV range. The difference gets larger, about 15%, with the increase in electron energy. The calculations performed by Jiang *et al*. [28] using the Additivity Rule (AR) are higher than current measurements at lower energies while both TCS agree (less than 4 % difference) in the energy range 0.50 – 1.50 keV. At higher energies the difference between the two sets becomes wider again. The TCS calculated by using the Energy Dependent Geometric Additivity Rule (EGAR) by the same group are in good agreement with present measurements at lower energies (0.10 – 1.00 keV) while EGAR calculations become lower with increasing electron energy. The calculated TCS by Jin-Feng *et al*. [20] are higher than present measurements at lower energies (as high as 46% at 0.10 keV). But this difference becomes smaller with the increasing electron energy and both sets seem to agree at higher energies.

3.2.4. Octafluorocyclobutane (c-C_4F_8)

A comparison of *c*-C_4F_8 TCS, reported by different experimental and theoretical groups, is presented in Figure 3.8. A summary of those TCS is given in Table 3.6 to study the deviation between them.

The first reported total cross section measurements of *c*-C_4F_8, in the intermediate electron energy range, was measured out by Nishimura in 1999 [29]. A more comprehensive study was done by the same group, Nishimura and Hamada, in 2007 [30]. Those TCS are different from current experiment by 10 - 30% with current measurements

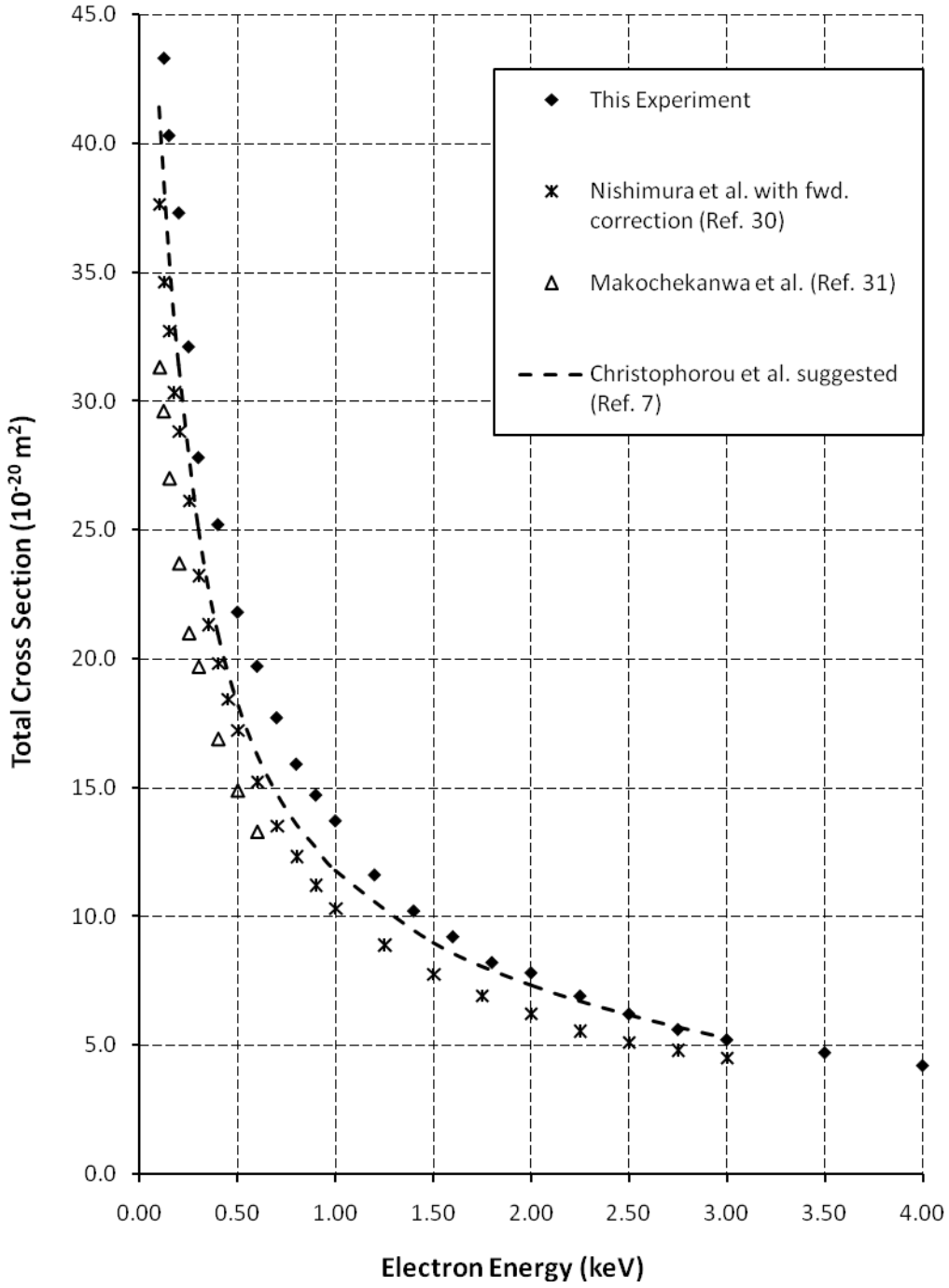

FIG. 3.8. A comparison of present *c*-C_4F_8 TCS with those produced by other experimental and theoretical groups. Dashed line represents theoretical TCS.

TABLE 3.6. The summary of experimental and theoretical total electron scattering cross section of *c*-C_4F_8 in units of 10^{-20} m^2.

	Experimental TCS				Theoretical TCS
Energy (keV)	This Exp.	Makochekanwa [31]	Nishimura [30] (measured)	Nishimura [30] (with fwd cor.)	Christophorou [7]
0.100		31.3	34.3	37.6	41.4
0.120		29.6			
0.125	43.3		31.4	34.6	
0.150	40.3	27.0	29.3	32.7	35.7
0.175			27.2	30.3	
0.20	37.3	23.7	25.8	28.8	31.4
0.25	32.1	21.0	23.3	26.1	
0.30	27.8	19.7	20.6	23.2	25.1
0.35			18.9	21.3	
0.40	25.2	16.9	17.5	19.8	21.0
0.45			16.2	18.4	
0.50	21.8	14.9	15.1	17.2	18.3
0.60	19.7	13.3	13.2	15.2	16.3
0.70	17.7		11.6	13.5	14.8
0.80	15.9		10.5	12.3	13.6
0.90	14.7		9.5	11.2	12.7
1.00	13.7		8.7	10.3	11.8
1.10					
1.20	11.6				
1.25			7.4	8.9	
1.40	10.2				
1.50			6.3	7.8	9.0
1.60	9.2				
1.75			5.5	6.9	
1.80	8.2				
2.00	7.8		4.9	6.2	7.4
2.25	6.9		4.3	5.5	
2.50	6.2		3.9	5.1	6.2
2.75	5.6		3.6	4.8	
3.00	5.2		3.4	4.5	5.3
3.50	4.7				
4.00	4.2				

being higher. The greatest difference is noticed at lower energies while the two measurements tend to agree in higher electron energies. Since measurements made by Nishimura and Hamada are heavily influenced by electrons scattered in the forward direction, they had to make a correction to overcome that problem. It's observed that this forward scattering correction made their measured total cross sections to increase by 10 - 33%. Although those corrected TCS are higher than their direct measurements, it is very hard to estimate the actual contribution due to forward-scattered electrons and hence the effect of that in the final result. As explained in Chapters One and Two, the present experiment has little of no influence due to electrons scattered in the forward direction. Therefore it is expected that present experiment yields higher TCS than that of Nishimura and Hamada. When compared with TCS of *c*-C_4F_8 measured by Makochekanwa *et al*. [31], present measurements are higher by 25 - 50%. But this comparison is limited for a very narrow energy range, 0.15 – 0.60 keV, due to the fact that Makochekanwa *et al*. made their measurements for low energy electrons (0.7 – 600 eV). Like Nishimura and Hamada [30], Makochekanwa *et al*. [31] also made corrections to their measured total cross sections to compensate for forward scattering electrons. There is not enough detail given in the literature about that correction; therefore it's very difficult to make a conclusion about the disparity between two measurements.

Christophorou and Olthoff [7] have summarized most of the studies carried out on electron interactions with *c*-C_4F_8 in their review paper. According to them, "the disparity between two sets of cross section measurements makes it difficult to recommend cross section values" and therefore they have compiled a set of "suggested" total cross sections, using the least squares average of two sets in the overlapping range and extending it to

other energies, to predict the TCS of electron scattering with *c*-C_4F_8. Those suggested values are in good agreement with current measurements in the higher electron energies, but about 10 - 15% lower at lower electron energies.

3.3. Relationship between TCS and Number of Electrons in Fluorocarbons and Hydrocarbons

It is interesting to analyze the relationship, if any, between TCS and number of electrons in the molecule. It has been agreed by many researches that the dominant factor in total electron scattering cross section, at intermediate energy range, in the number of electrons or the number of "scattering centers" of the target molecule. In this analysis, the ratio of fluorocarbons TCS, measured in this experiment, is compared with corresponding ratio of the number of electrons in each molecule. Also similar ratios for hydrocarbon TCS, measured previously in this laboratory [38, 43], are calculated for a better comparison. Table 3.7 shows the calculated TCS ratios (the average of TCS at all electron energies) for both fluorocarbons and hydrocarbons, with corresponding number of electron ratios.

TABLE 3.7. The average TCS ratios of Fluorocarbons and Hydrocarbons with their number of electrons ratios.

Molecule ratio	TCS ratio (Avg. of all energies)	Number of electrons ratio
C_4F_8 / C_2F_6	1.5	1.4
C_4F_8 / CF_4	2.5	2.3
C_2F_6 / CF_4	1.6	1.6
C_4H_8 / C_2H_6	1.7	1.8
C_4H_8 / CH_4	3.2	3.2
C_2H_6 / CH_4	1.9	1.8

When comparing TCS ratios with number of electron ratios, the following two arguments can be made by analyzing the data in Table 3.7:

1. As expected before, individual TCS ratios came out to be very close to their number of electron ratios. Therefore it is reasonable to assume that the total electron scattering cross section of heavy molecules, at intermediate energy range, is dominated by the number of electrons of the target molecule. Since all the molecules considered in this study consist of a large number of electrons, the target electron beam is primarily scattered by those electrons.
2. When carefully analyzing the data in Table 3.7, it is evident that there is some difference between TCS ratio and electrons ratio, although those two are close to each other. This difference is more evident when the ratio involves *c*-C_4F_8 molecule. When analyzing the structure of molecules, it can be seen that all other molecules used in this study are linear type molecules while *c*-C_4F_8 (Octafluorocyclobutane) is a cyclic type molecule. Since the TCS is also considered as a measure of the *effective surface area* of the target molecule presented to an energetic beam of electrons, it is expected that the structure of the module should also affect the measured TCS.

Based on the results obtained from the above analysis it is fair to conclude that the number of electrons in a heavy molecule plays the main role in the TCS of that molecule, in the intermediate electron energy range. Also the structure of a molecule has some role to play in the TCS of that particular molecule too.

3.4. Development of an Emperical Formula to Predit TCS of linear Flurocarbons

3.4.1. Introduction to the Empirical Formula

It is very important to have some type of a formula which can be used to calculate the TCS as functions of electron energy and number of individual atoms in the target molecule. As discussed in Chapter One, some groups tried to achieve this in several different ways. As a result of those works there are few theoretical models and emperical formulas available for TCS calculations. Since almost all the theoretical models depend on several simplyfying ssumptions and involve complex calculations, TCS calculated using those are not in good agreement with laboratory measuremensts. Also there is only one empirical formula available in the literature which can be used to calculate TCS of fluorocarbons at intermediate energies. Because that formula, proposed by Garcia *et a*l. [25], is primarily developed for molecules with 10 – 22 electrons, it is not the ideal formula to predict TCS measured in this experiment.

3.4.2. Methodology

One of most widely used formulas in expressing the total scattering cross section, as a function of electron energy, is the formula proposed by Joshipura and Vinodkumar [44] and is given by;

$$\sigma = AE^{-B} \tag{3.1}$$

Here the TCS (σ) is expressed in the units of the Bohr radius squared (a_0^2), energy E in keV and A, B are fitting parameters depending on properties of the target gas. According to this equation, the graph of *ln (σ) vs ln (E)* should be a straight line. Therefore as the first step of developing an empirical formula, *ln (σ) and ln (E*) are plotted against each

other for all the gases used in this study. Figure 3.9 shows the graph of *ln (σ) vs ln (E)* for CF_4 while Figures 3.10, 3.11 and 3.12 are that of CHF_3, C_2F_6 and *c*-C_4F_8, respectively.

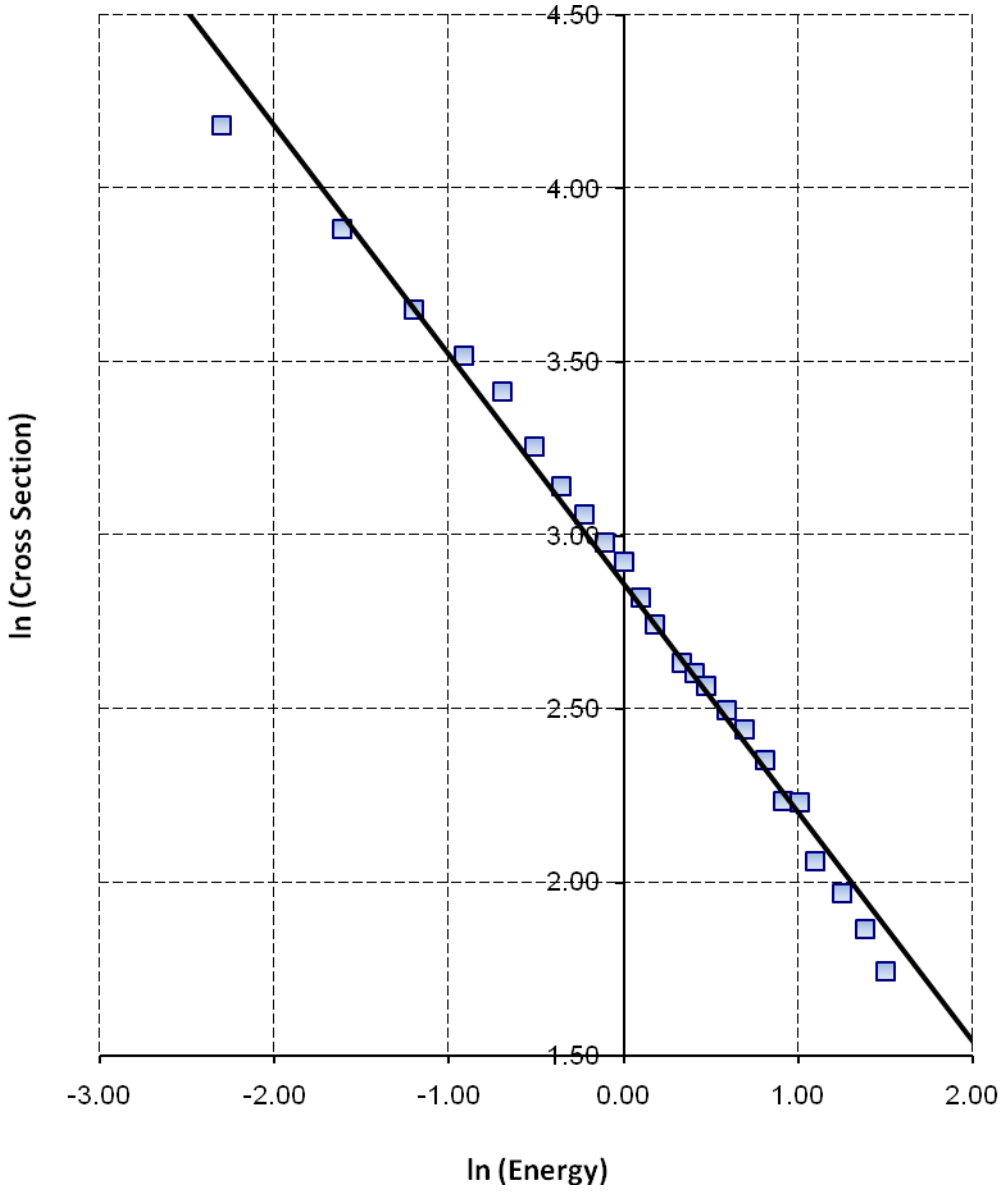

FIG 3.9. The graph of *ln (σ) vs ln (E)* for CF_4 for the energy range 0.10 – 4.50keV. Energy (E) is in units of keV and the cross section (σ) is in units of Bohr radius squared. The solid line is the linear regression line (best fit line) for experimental data.

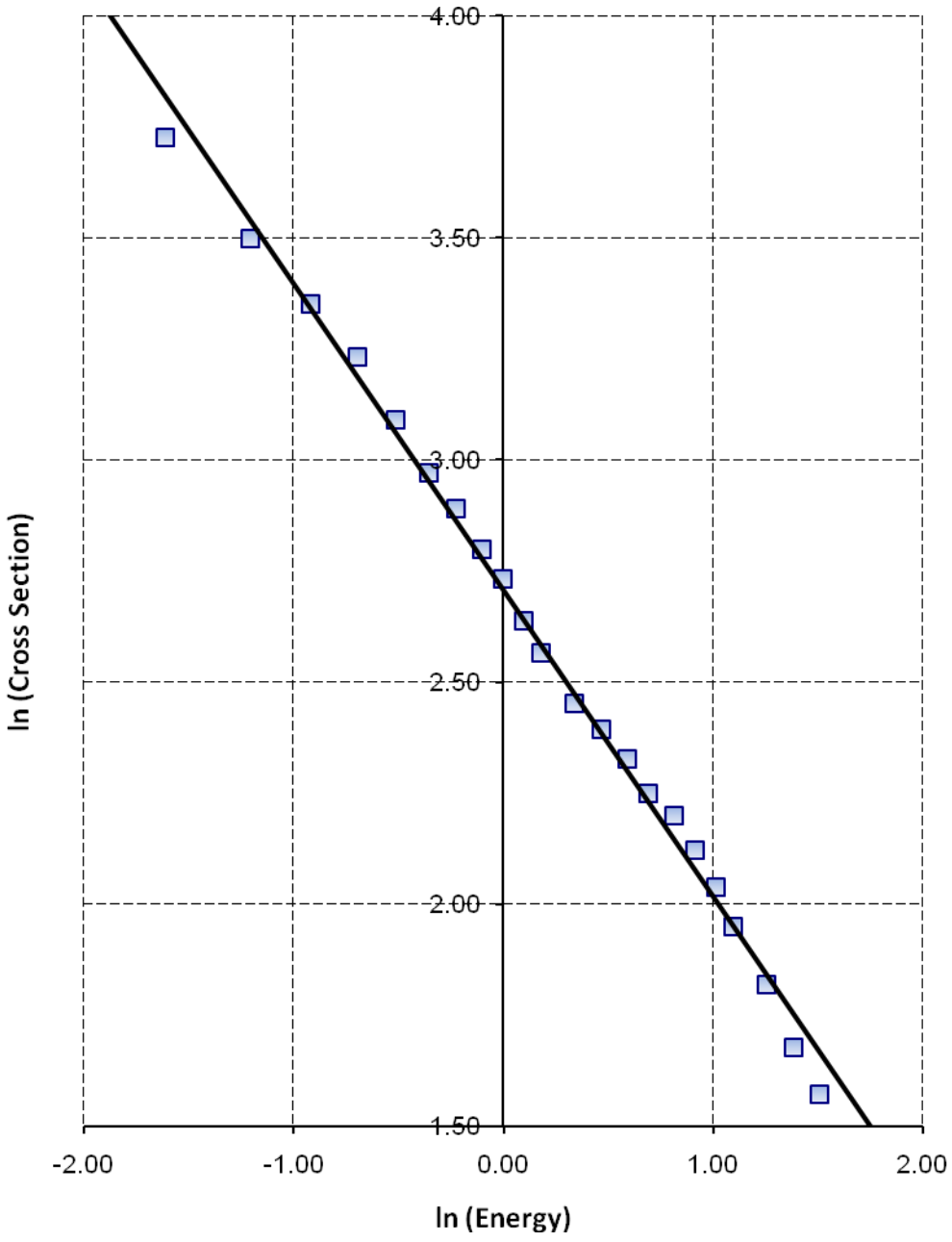

FIG 3.10. The graph of *ln (σ) vs ln (E)* for CHF_3 for the energy range 0.20 – 4.50 keV. Energy (E) is in units of keV and the cross section (σ) is in units of Bohr radius squared. The solid line is the linear regression line (best fit line) for experimental data.

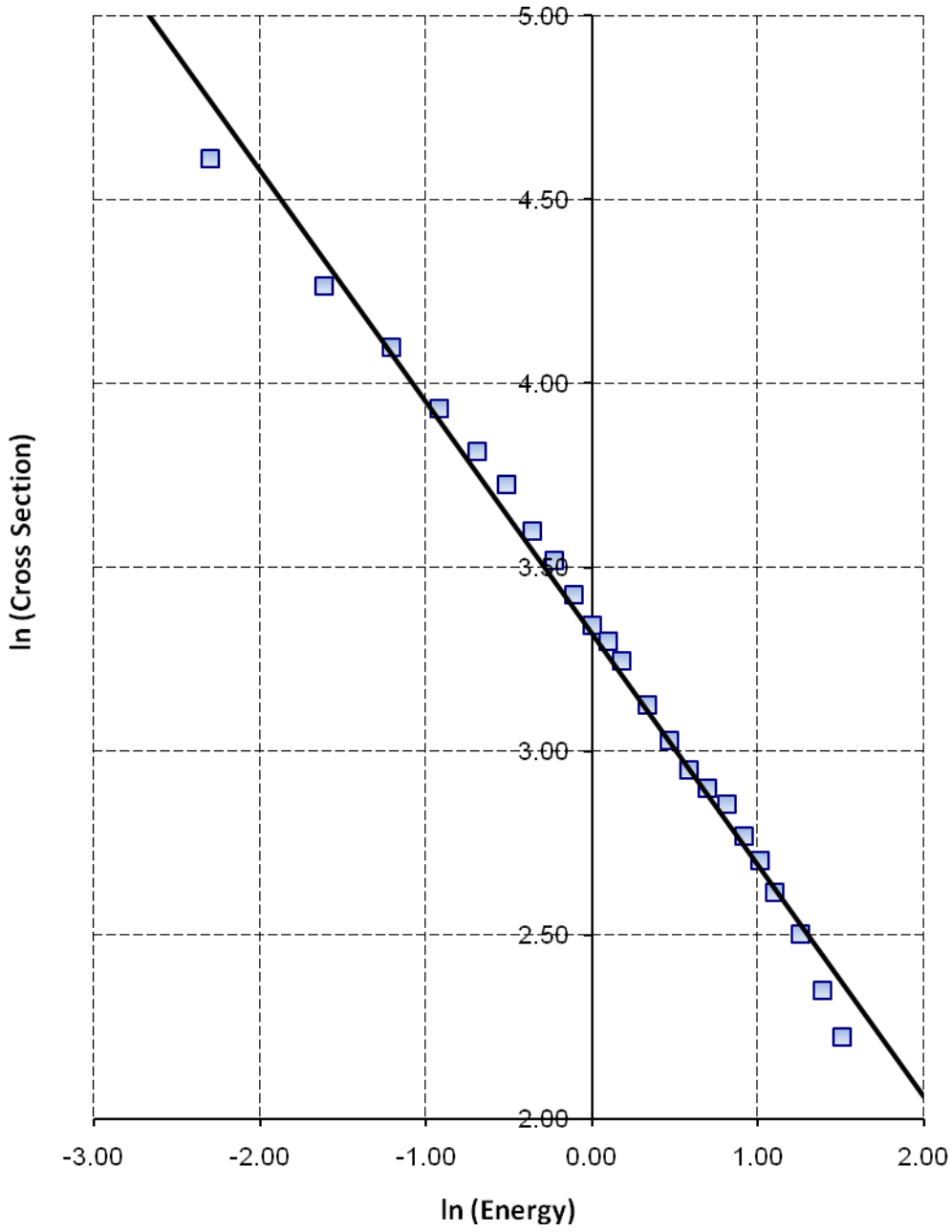

FIG 3.11. The graph of *ln (σ) vs ln (E)* for C_2F_6 for the energy range 0.10 – 4.50 keV. Energy (E) is in units of keV and cross section (σ) is in units of Bohr radius squared. The solid line is the linear regression line (best fit line) for experimental data.

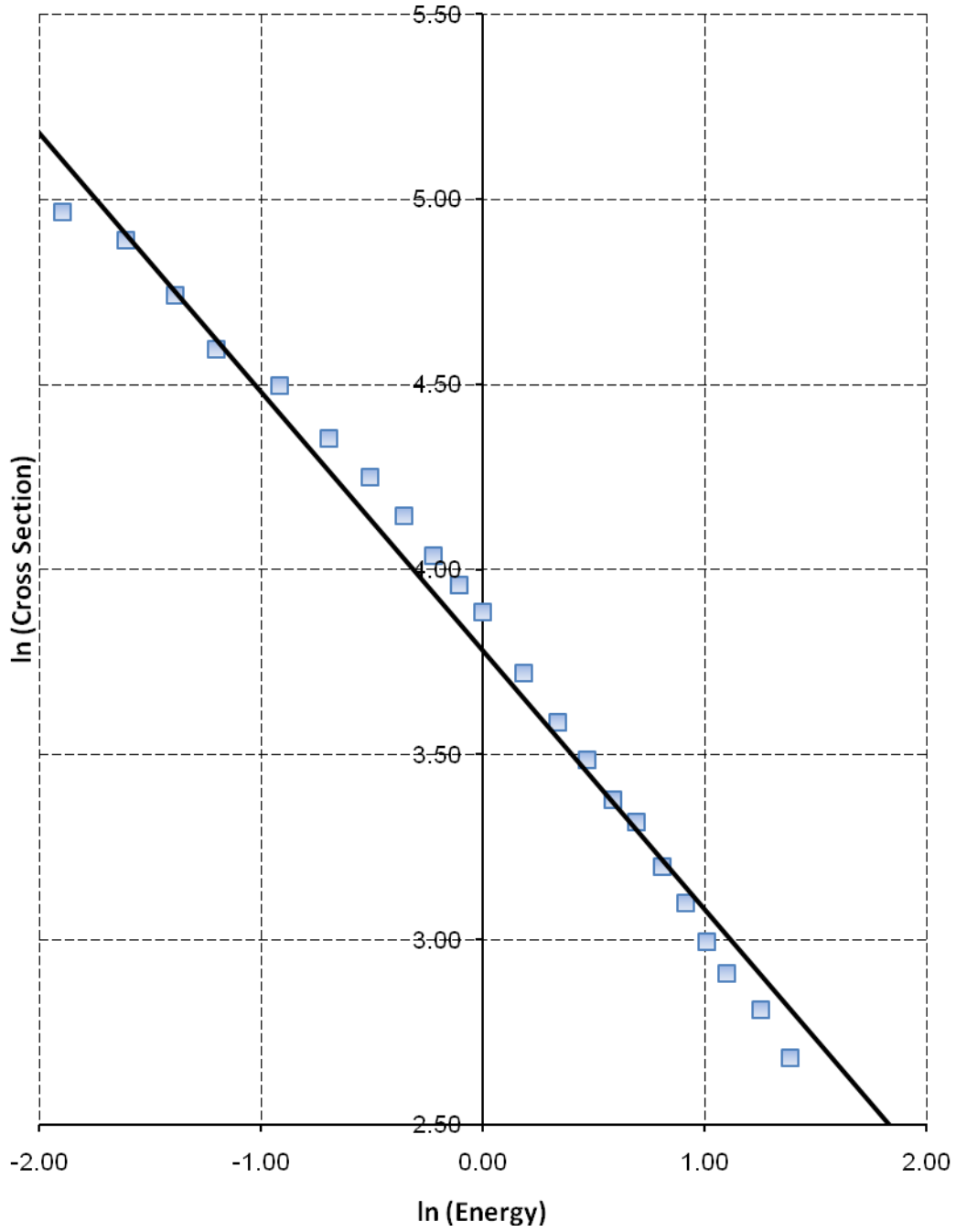

FIG 3.12. The graph of *ln (σ) vs ln (E)* for *c*-C_4F_8 for the energy range 0.10 – 4.00 keV. Energy (E) is in units of keV and cross section (σ) is in units of Bohr radius squared. The solid line is the linear regression line (best fit line) for experimental data.

As evident from those plots, measured TCS of CF_4, CHF_3 and C_2F_6 are in good agreement with the formula proposed by Joshipura and Vinodkumar [44]. Therefore it is reasonable to conclude that, in general, the TCS of the above mentioned fluorocarbons are proportional to some power of the incident electron energy. The same pattern is also observed for linear alkanes in a previous work done in this laboratory [38, 43].

Further analysis shows that the behavior of log-log plots tend to deviate from the linear regression line at very low energies (< 0.30 keV) and at higher energies (> 3.50 keV). As discussed in Chapter One, mechanisms governing scattering processes of electron-molecule scattering at lower energies are different from those at higher energies the observed deviation of log-log plots at lower and higher energy ends is justified. After omitting those low and high energy data points a more accurate best fit line ($R^2 > 99\%$) for each molecule was obtained. Therefore the proposed empirical formula is developed for 0.30 – 3.50 keV energy range. It's also noticed that the log-log plot of *c*-C_4F_8 is not as linear as in other gases with a best fit line of $R^2 \sim 98\%$. As observed in the previous TCS to number of electrons ratio analysis given in Table 3.7, the deviation of the linearity in Figure 3.12 could be due to the cyclic structure of the *c*-C_4F_8 which is different from other molecules used in this study. Therefore it is decided to develop the empirical formula to predict only the TCS of linear fluorocarbons.

The second idea of developing this empirical formula is to express TCS as a function(s) of the number of target atom(s) and hence number of electrons (Z) in that molecule. As discussed in the Chapter One, in several previous studies it was shown that the TCS increases with the increasing number of target electrons. Thus the TCS measured in this study are considered as a linear function of number of fluorine, carbon

and hydrogen atoms in that particular molecule. To satisfy the both of those conditions, it is proposed that the TCS (σ_T) of a linear fluorocarbon is given by;

$$\sigma_T = N_F \sigma_F + N_C \sigma_C + N_H \sigma_H \quad (3.2)$$

where N_F, N_C and N_H are the number of fluorine atoms, number of carbon atoms and number of hydrogen atoms, respectively, in the target molecule. The parameters σ_F, σ_C and σ_H, respectively, are defined as the fluorine atom cross section, carbon atom cross section, and hydrogen atom cross section at a given energy. Numerical values of the first two parameters (σ_F and σ_C) are obtained by analyzing the cross sections measured in this experiment, as explained in the next paragraph. Because of insufficient data in this experiment to carry out an independent analysis on hydrogen atom cross section (σ_H), a value from a previous work done in this lab on hydrogen atom cross section [38] is used as the σ_H when the empirical formula is used to reproduce TCS of CHF_3.

The calculation of a single fluorine atom cross section is done in the following manner. The cross section of a CF_2 group is obtained by subtracting the CF_4 cross section from C_2F_6 cross section. Then it is subtracted from the CF_4 cross section to calculate the cross section of a F_2 group or two fluorine atoms. Finally the cross section of a single fluorine atom (σ_F) is calculated by taking a half of the F_2 cross section. This procedure is done for electron energy range 0.30 – 3.50 keV to obtain the best fit curve for the fluorine atom cross section. The variation of the fluorine atom cross section with the electron energy is plotted in the Figure 3.13. The best fit curve for the fluorine cross section agrees with the expected behavior and hence is expressed as a power of the electron energy.

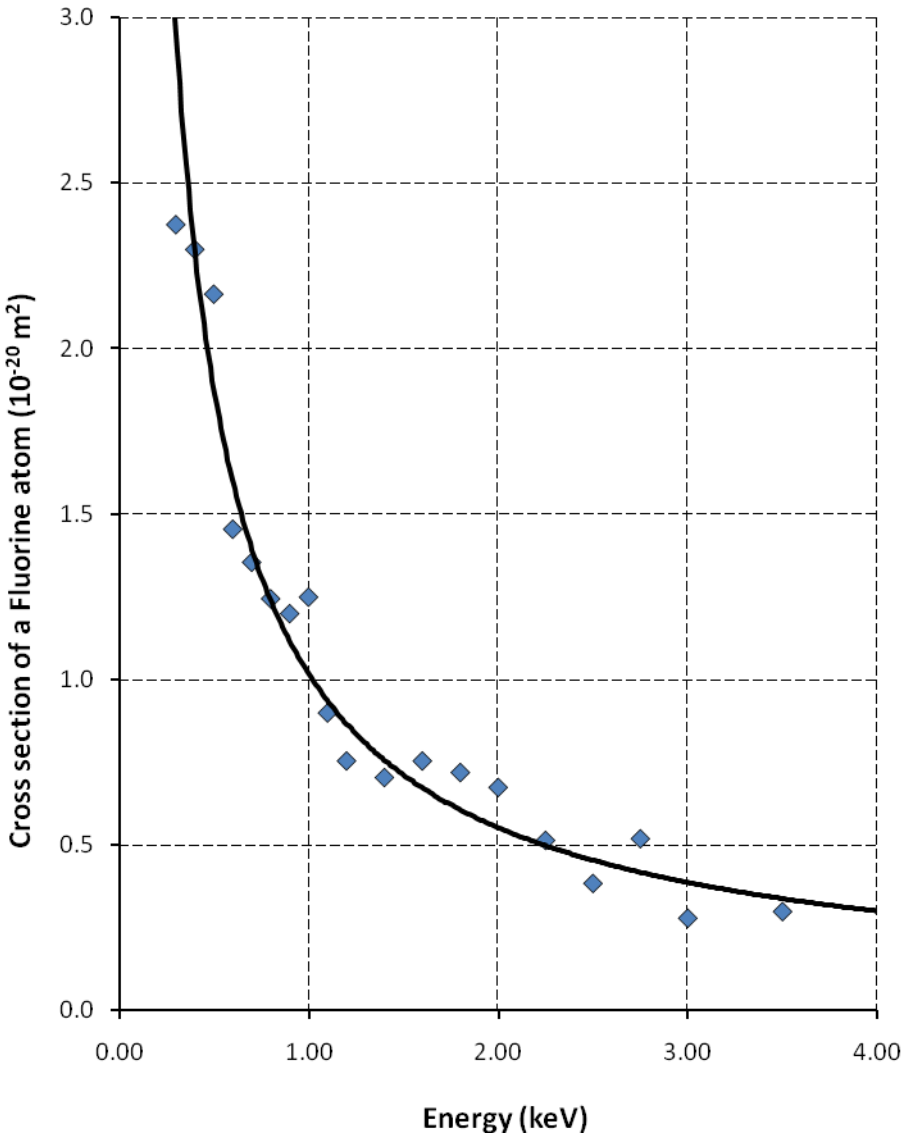

FIG 3.13. Variation of the total cross section of a Fluorine atom for the energy range 0.30 – 3.50 keV. The solid line is the best fit for plotted data.

The carbon atom cross section (σ_C) is obtained by substituting the previously calculated fluorine atom cross section into the CF_4 cross section. This is also done for all electron energies to observe the behavior of $\sigma_{C,}$ as a function of the electron energy. But interestingly the contribution from a carbon atom cross section to the total cross section remains roughly a constant for all electron energies considered in this study. This

behavior is different from the observed behavior for carbon atom cross section in a previous study [38, 43] where the carbon atom cross section of linear alkanes is also expressed as a function of the energy. Although this seems somewhat strange, after considering the fact that the fluorine atoms dominate the number of scattering centers, more than a 5:1 ratio in fluorocarbons used in this study, it is reasonable to assume that the carbon atoms in these fluorocarbons are shielded by fluorine atoms. Therefore it is reasonable to assume that the contribution form a carbon atom to the total cross section of linear fluorocarbons remains roughly a constant at the intermediate electron energy range.

After combining individual contributions due to fluorine and carbon atoms, the equation 3.2 can be rewritten as;

$$\sigma_T = 1.02\ E^{-0.88}\ N_F + 0.79\ N_C \qquad (3.3)$$

where, σ_T is the total electron scattering cross section of the linear fluorocarbon in interest, E is the energy of the incoming electrons in the units of keV, N_F and N_C are the number of fluorine and carbon atoms in that fluorocarbon.

Since it is necessary to account for the hydrogen atom cross section (σ_H) for the calculation of CHF_3 TCS, σ_H obtained from a previous study [38, 43] is used for that purpose. It should be noted that the value of σ_H came from a totally different study done in this laboratory, on linear alkanes, and therefore it is difficult to make a firm conclusion about the behavior of the hydrogen cross section in linear fluorocarbons. After combining the hydrogen atom cross section (σ_H), the equation 3.1 can be expressed as;

$$\sigma_T = 1.02\ E^{-0.88}\ N_F + 0.28\ E^{-0.81}\ N_H + 0.79\ N_C \qquad (3.4)$$

where, σ_T is the total electron scattering cross section of the linear fluorocarbon in interest, E is the energy of the incoming electrons in the units of keV, N_F, N_H and N_C are the number of fluorine, hydrogen and carbon atoms in that fluorocarbon.

3.4.3. Comparison of TCS Predicted by the Empirical Formula with Measured TCS

In this section TCS of CF_4, C_2F_6 and CHF_3, measured in this study, are compared with those predicted from the empirical formula (Eq. 3.3). The comparison of CF_4 empirical TCS with present measurements and those in the literature is given in Figure 3.14. Similar comparisons for C_2F_6 and CHF_3 are shown in Figures 3.15 and 3.16, respectively.

When comparing the total electron scattering cross sections predicted by the empirical formula (Eq. 3.3) with those measured in this study for CF_4, it is observed that the predicted TCS only differ by 0 - 7 % with the measured TCS. Also empirical TCS are within 0 - 10 % difference with those reported by Zecca *et al*. [12] and Manero *et al*. [15], when the energy is below 2.00 keV. When the energy is higher than 2.00 keV, TCS measured by Zecca *et al*. are about 7 - 20 % lower than the empirical formula calculations. The difference between TCS measured by Nishimura *et al*. [16] and Sueoka *et al*. [13] are about 10-20 % lower than those predicted by the Eq. 3.3. Probable causes for this difference are explained in the previous section. Among theoretical calculations, TCS predicted by Antony *et al*. [21] are in very good agreement with the present empirical calculations up to 1.20 keV. At energies higher than that, TCS calculated by Antony *et a*l. are about 10 - 20 % lower than the present empirical values. The TCS predicted by Jiang *et al*. [18] and Jin-Feng *et al*. [20] are significantly higher than those obtained from Eq. 3.3 and also from all experimental CF_4 TCS.

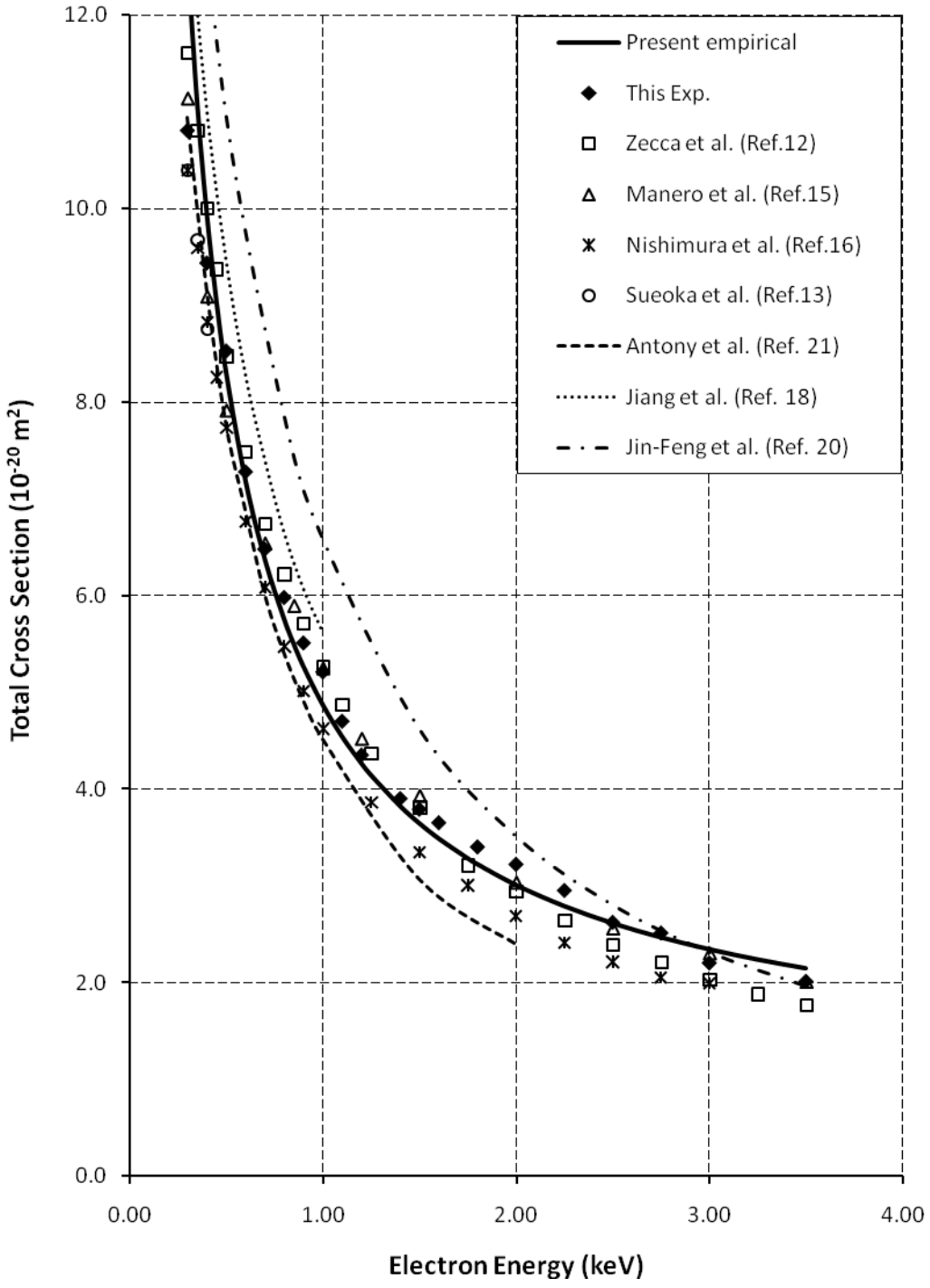

FIG 3.14. A comparison of empirically calculated CF_4 TCS with the present measurements and those in the literature. The solid line represents the predictions of the empirical formula and dashed lines represent other theoretical TCS.

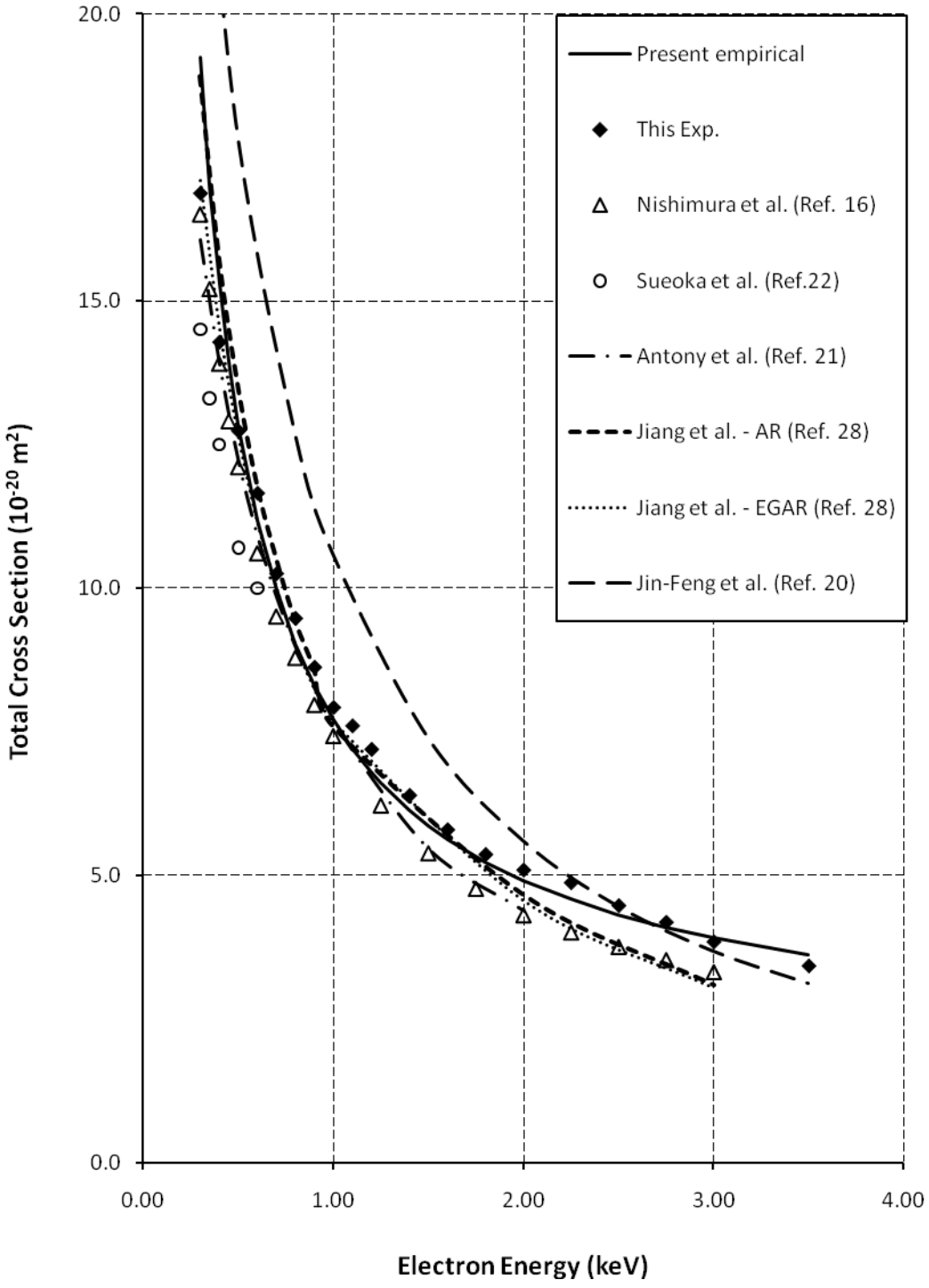

FIG. 3.15. A comparison of empirically calculated C_2F_6 TCS with the present measurements and those in the literature. The solid line represents the predictions of the empirical formula and dashed lines represent other theoretical TCS.

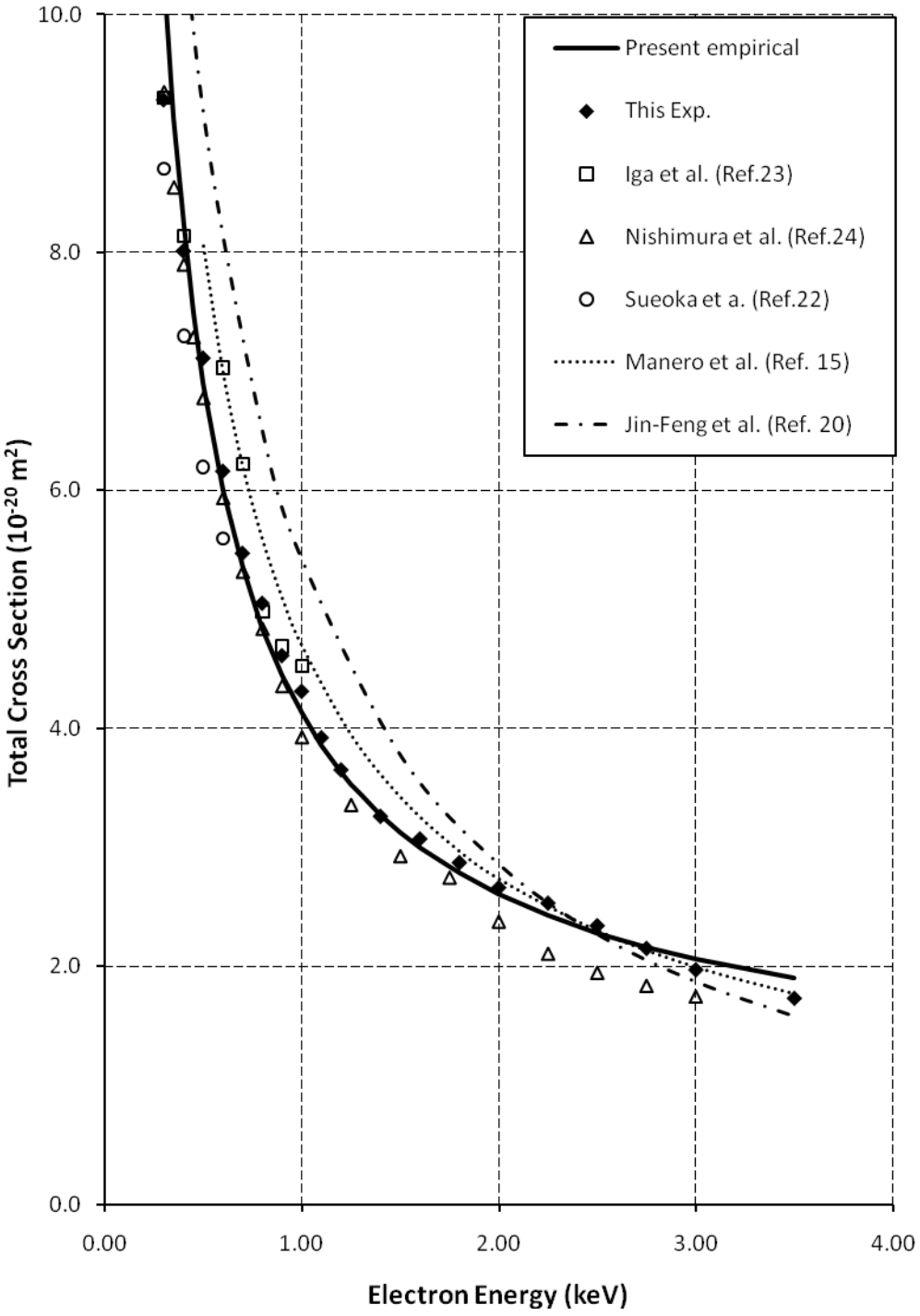

FIG. 3.16. A comparison of empirically calculated CHF_3 TCS with the present measurements and those in the literature. The solid line represents the predictions of the empirical formula and dashed lines represent other theoretical TCS.

The TCS obtained for C_2F_6 are also in very good agreement, about 0 - 7 % difference, with the predictions of empirical formula. Experimental TCS reported by Nishimura *et al*. [16] and Sueoka *et al*. [27] are about 10 - 15 % lower than empirical formula predictions. Both Additivity Rule (AR) and Energy Dependent Additivity Rule (EAGR) calculations of C_2F_6 TCS reported by Jiang *et al*. [28] are in good agreement (less than 5% difference) with the present calculations for 2.00 keV and below energies. The difference between two sets increases for energies higher than 2.00 keV with present calculations being higher. The predictions made by Antony *et al*. [21] are also in a good agreement with the present empirical formula since the difference between two sets is less than 5 % at lower energies. As in the CF_4 case, the TCS predicted by Jin-Feng *et al*. [20] are significantly higher than those obtained from Eq. 3.2 up to 2.00 keV, while the two calculations are in agreement with each other at higher energies.

The predicted TCS for CHF_3 (Eq. 3.4) are only differed by 0 - 5 % from the experimental measurements up to 3.00 keV. At 3.50 keV, the difference becomes the highest (10 %). Also the present empirical formula cross sections are within 10 % difference from those measured by Iga *et al* [23], Nishimura et al. [24] and Sueoka *et al*. [22] for the electron energy below 2.00 keV. When the energy is 2.00 keV and above, present predictions are about 15 - 20 % higher than those reported by Nishimura et al. The TCS calculated by Manero *et al*. [15], using their empirical formula, are 0 - 15 % different from present calculations with the highest difference is observed at lower electron energies. Similar to the C_2F_6 gas, the TCS predicted by Jin-Feng *et al*. [20] are significantly higher than those obtained from Eq. 3.4 for energies below 2.00 keV while two calculations are in agreement with each other at around 2.50 keV. At energies higher

than 3.00 keV, the predictions by Jin-Feng *et al*. are lower than those obtained from Eq. 3.4.

3.4.4. Prediction of C_3F_8 and C_4F_{10} Total Cross Sections using the Empirical Formula

Since one of the ideas of developing the empirical formula is to predict TCS of linear fluorocarbons with single carbon-carbon bonds, it is necessary to use it to predict TCS of other fluorocarbons to check the validity of the formula. Therefore the TCS of C_3F_8 and C_4F_{10} gases are calculated for the energy range 0.30 - 3.00 keV, using the present empirical formula. Those predictions are given in Table 3.8. A comparison of predicted TCS of C_3F_8 with those available in literature is shown in Figure 3.17. A similar comparison for C_4H_{10} is shown in Figure 3.18.

As is evident from Figure 3.17, the present empirical formula is capable of prediction C_3F_8 cross sections with 1 - 10 % difference when compared to those measured by Tanaka *et al*. [32] and Nishimura *et al*. [16]. As discussed before, each of these groups' experimental technique is subjected to forward scattering electrons and hence their measurements are somewhat lower than the TCS measured in other laboratories. As can be seen in Figures 3.14, 3.15 and 3.16, the TCS reported by both Nishimura and co-workers and Tanaka and co-workers are always lower than the TCS produced in the present experiment. Therefore it is reasonable to assume that the difference between the present empirical TCS and cross sections reported by Nishimura *et a*l. [16] and Tanaka *et al*. [32] is due to the forward scattering error in those two groups' experimental method. Among theoretical TCS of C_3F_8 available in the literature, predictions made by Antony *et al*. [21] are in a good agreement (less than 6 % difference) with the present calculations. The TCS calculated by Jiang *et al*. [28], using both the

Additivity Rule (AR) and Energy Dependent Additivity Rule (EAGR), only differ from present predictions by 0 - 5 % for electron energy below 2.00 keV. The difference between groups becomes 15 - 20 % at higher energies.

There is only one reported C_4F_{10} total electron scattering cross section data (experimental or theoretical) in the literature. When compared with the TCS reported by Makochekanwa *et al*. [33], present predictions came out to be 15 -20 % higher. Since their technique of measuring the TCS is affected by the electrons scattering in the forward direction, it is reasonable to expect those measurements to be somewhat lower than the actual TCS. Also due to the tact that Makochekanwa *et al*. reports their TCS only up to 0.80 keV, a complete comparison between two TCS sets is impossible.

TABLE 3.8. Predicted total electron scattering cross section for C_3F_8 and C_4F_{10}, using the empirical formula, in units of 10^{-20} m^2

Energy (keV)	C_3F_8	C_4F_{10}
0.30	25.7	32.3
0.40	20.4	25.7
0.50	17.1	21.6
0.60	14.9	18.8
0.70	13.3	16.8
0.80	12.1	15.3
0.90	11.1	14.0
1.00	10.3	13.0
1.20	9.1	11.5
1.40	8.2	10.4
1.60	7.5	9.6
1.80	7.0	8.9
2.00	6.6	8.4
2.25	6.1	7.8
2.50	5.8	7.4
2.75	5.5	7.0
3.00	5.2	6.7
3.50	4.8	6.2

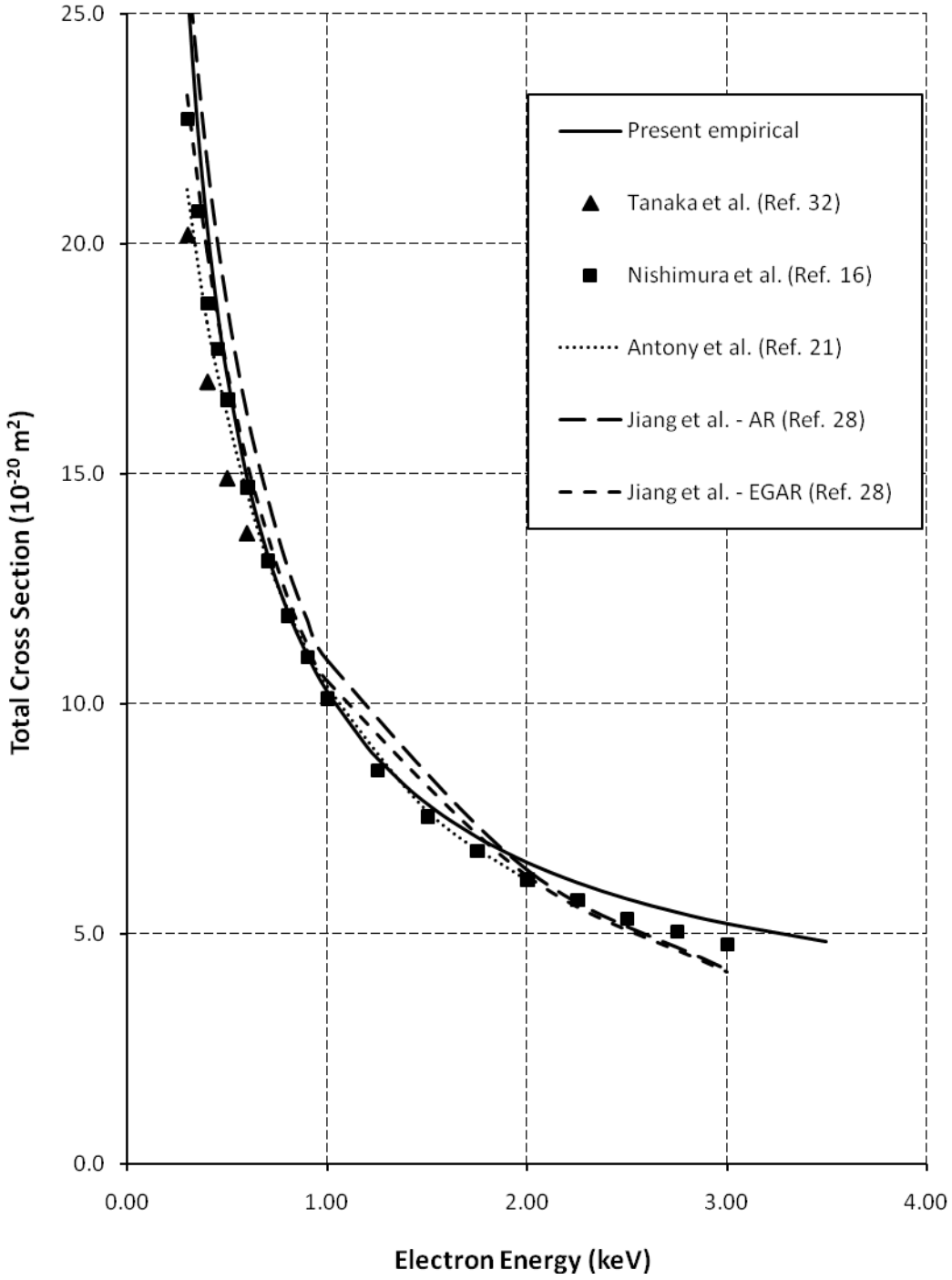

FIG. 3.17. A comparison of empirically calculated C_3F_8 TCS with those in the literature. The solid line represents the preditions of the emperical formula and dashed lines represent other theoretical TCS.

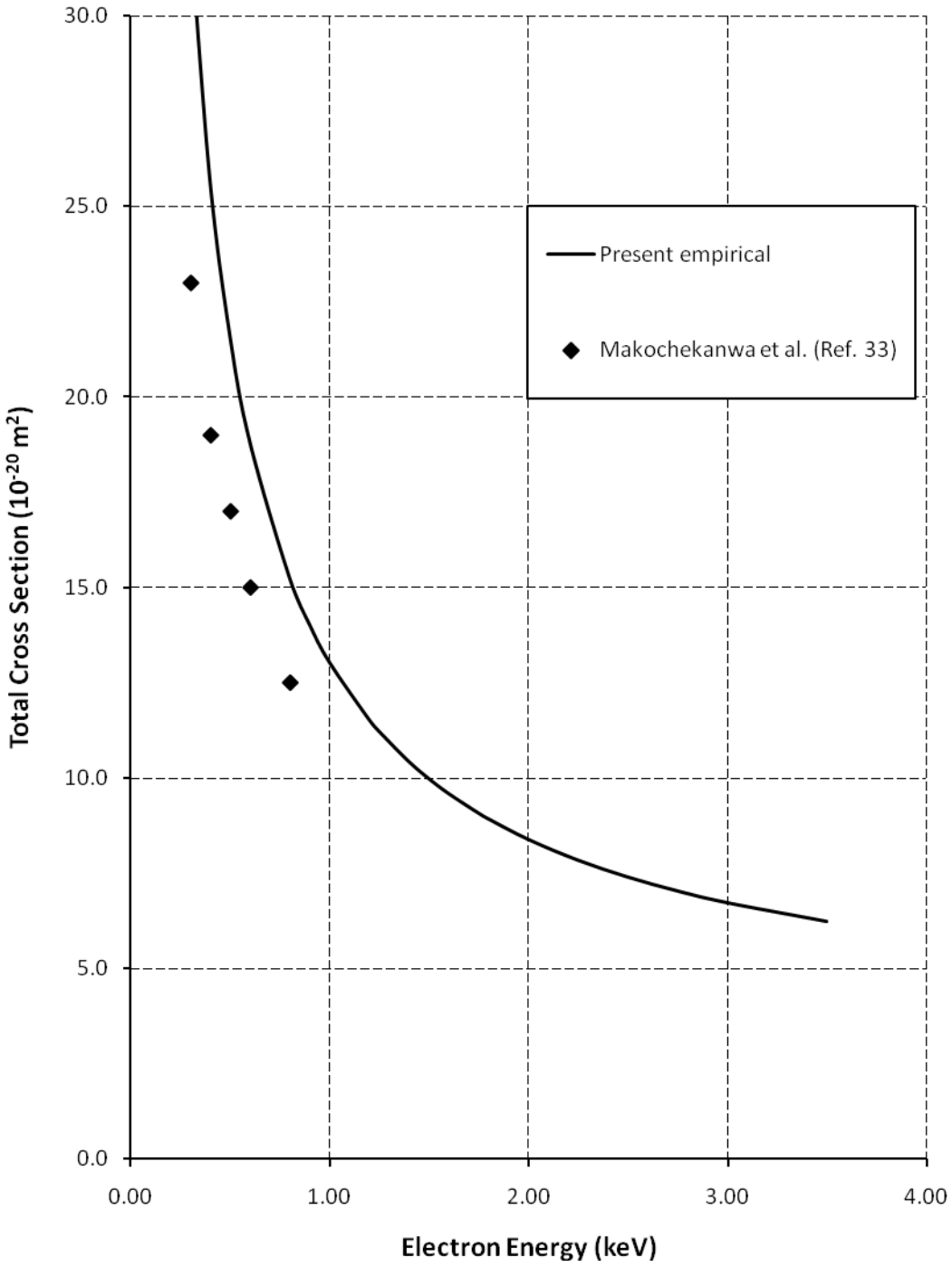

FIG. 3.18. A comparison of empirically calculated C_4F_{10} TCS with those in the literature. The solid line represents the preditions of the emperical formula.

CHAPTER FOUR

Conclusions

The total electron scattering cross sections for CF_4, CHF_3, C_2F_6, and *c*-C_4F_8 were measured for the intermediate electron energy range (0.10 – 4.50 keV) using the linear transmission technique. Using the measured cross sections, a simple empirical formula was developed to predict the total cross sections of linear fluorocarbons as a function of the electron energy and the number of individual atoms in the target molecule.

The present cross section measurements of all gases agree with experimental TCS reported by other groups with 0-20%. The present TCS are always higher than those reported by two experimental groups [13, 16, 22, 24, 27, 30, 31]. Total cross section measurements made by those two are affected by the forward-scattered electrons and therefore those TCS are always lower than the actual TCS. Also the present TCS agree (0-15% difference) with theoretical TCS reported in [15, 18, 21, 28] by several authors. The TCS calculated in [20] are always higher (15-45%) than the present TCS and also other experimental TCS in the literature.

An empirical formula was developed to predict TCS of linear fluorocarbons in the energy range 0.30 – 3.50 keV. The TCS obtained from the empirical formula are within 0-10% from the present measurements with the highest difference is observed at the lower and higher ends of the energy range. When the empirical formula was used to predict C_3F_8 and C_4F_{10} cross sections, which were not measured in this study, the predictions came out to be in good agreement with C_3F_8 TCS available in the literature. There are insufficient data in the literature for C_4F_{10} to make a meaningful comparison.

REFERENCES

[1] L. G. Christophorou, *Electron-Molecule Interactions and Their Applications* (Academic, Florida, 1984).

[2] S. Trajmar, D. F. Register, and A. Chutjian, *Electron Scattering by Molecules 2: Experimental Methods and Data*, (ELSEVIER SCIENCE BV, Amsterdam, 1983).

[3] K. H. Becker, W. McCurdy, and T. Ornaldo, work shop on *Electron Driven Processes: Scientific Challenges and Technological Opportunities* (March, 2000).

[4] L. G. Christophorou, J. K. Olthoff, and M. V. V. S. Rao, J. Phys. Chem. Ref. Data **25**, 1341 (1996).

[5] L. G. Christophorou, J. K. Olthoff, and M. V. V. S. Rao, J. Phys. Chem. Ref. Data **26**, 1 (1997).

[6] L. G. Christophorou and J. K. Olthoff, J. Phys. Chem. Ref. Data **27**, 1 (1998).

[7] L. G. Christophorou and J. K. Olthoff, J. Phys. Chem. Ref. Data **30**, 449 (2001).

[8] B. Bederson and L. J. Kiefer, Rev. Mod. Phys. **43**, 601 (1971).

[9] L. G. Christophorou and J. K. Olthoff, J. Phys. Chem. Ref. Data **28**, 967 (1999).

[10] L. G. Christophorou and J. K. Olthoff, App. Surf. Sci. **192**, 309 (2002).

[11] C. Szmytkowski, A. M. Krzysztofowicz, P. Janicki, and L. Rosenthal, Chem. Phys. Lett. **199**, 191 (1992).

[12] A. Zecca, G.P. Karwaz, and R. Brusa, Phys. Rev. A **46**, 3877 (1992).

[13] O. Sueoka, S. Mori, and A. Hamada, J. Phys. B: At. Mol. Opt. Phys. **27**, 1453 (1994).

[14] W. M. Ariyasinghe, Rad. Phys. Chem. **68**, 79 (2003).

[15] F. Manero, F. Blanco, and G. Garcia, Phys. Rev. A **66**, 032713 (2002).

[16] H. Nishimura, F. Nishimura, Y. Nakamura, and K. Okuda, J. Phys. Soc. Jpn. **72**, 1080 (2003).

[17] K. L. Baluja, A. Jain, V. D. Martino, and F. A. Gianturco, Europhys Lett. **17**, 139 (1992).

[18] Y. Jiang, J. Sun, and L. Wan Phys. Rev. A **52**, 398 (1995)

[19] E. Bruche, Ann. Phys. (Leipzing) **1**, 93 (1929).

[20] S. Jin-Feng, X. Bin, L. Yu-Fang, and S. De-Heng, Chin. Phys. **14**, 1125 (2005).

[21] B. K. Antony, K. N. Joshipura, and N. J. Mason, J. Phys. B: At. Mol. Opt. Phys. **38**, 189 (2005).

[22] O. Sueoka, H. Takaki, A. Hamada, H. Sato, and M. Kumara, Chem. Phys. Lett. **288**, 124 (1998).

[23] I. Iga, P. R. Pinto, and M. G. P. Homem, *International Symposium on Electron-Molecule Collisions and Swarms, Tokyo* (1999).

[24] H. Nishimura and Y. Nakamura, J. Phys. Soc. Jpn. **74**, 1160 (2005).

[25] G. Garcia and F. Manero, Chem. Phys. Lett. **280**, 419 (1997).

[26] C. Szmytkowski, P. Mozejko, G. Kasperski, and E. P. Denga, J. Phys. B: At. Mol. Opt. Phys. **33**, 15 (2000).

[27] O. Sueoka, C. Makochekanwa, and H. Kawate, Nucl. Instr. Meth. Phys. Res. B 192, 206 (2002).

[28] Y. Jiang, J. Sun, and L. Wan, Phys. Rev. A **62**, 062712 (2000).

[29] H. Nishimura, *International Symposium on Electron-Molecule Collisions and Swarms, Tokyo* (1999).

[30] H. Nishimura and A. Hamada, J. Phys. Soc. Jpn. **76**, 014301 (2007).

[31] C. Makochekanwa, O. Sueoka, M. Kimura, M. Kitajima, and H. Tanaka, Phys. Rev. A **71**, 032717 (2005).

[32] H. Tanaka, Y. Tachibana, M. Kitajima, O. Sueoka, H. Takaki, A. Hamada, and M. Kimura, Phys. Rev. A **59**, 2006 (1999).

[33] C. Makochekanwa, O. Sueoka, and M. Kimura, *Gaseous Dielectrics X*, 181 (2004).

[34] H. J. Blaauw, R. W. Wagenaar, D. H. Barends, and F. J. de Heer, J. Phys. B **13**, 359 (1980).

[35] W. M. Ariyasinghe and D. Powers, Phys. Rev. A **66**, 052716 (2002).

[36] T. T. Wijerathne, *M.S. Thesis*, Baylor University, Waco, TX (2004).

[37] C. P. Goains, *Ph. D. Disser*tation, Baylor University, Waco, TX (2004).

[38] P. Wickramarachi, *M.S. Thesis*, Baylor University, Waco, TX (2006).

[39] Kimball Physics EGG-3101, *Electron Gun Instruction Manual*, Kimball Physics Inc., Wilton, NH.

[40] MKS Baratron 626 A, *Capacitance Manometer Instructions Manual*, MKS Instruments, Andover, Massachusetts.

[41] Comstock AC-902, *Electro Static Analyzer Instruction Manual*, Comstock Inc., Oak Ridge, Tennessee.

[42] P. Guo, A. Ghebremedhin,W. M. Ariyasinghe and D. Powers, Phys. Rev. A **51**, 2117 (1995)

[43] W. M. Ariyasinghe, P. Wickramarachi, and P. Palihawadana, Nucl. Instr. Meth. Phys. Res. B **259**, 841 (2007).

[44] K. N. Joshipura and M. Vinodkumar, Pramana **47**, 57 (1996).

BIBILIOGRAPHY

Antony B. K., Joshipura K. N., and Mason N. J., J. Phys. B: At. Mol. Opt. Phys. **38**, 189 (2005).

Ariyasinghe W. M. and Powers D., Phys. Rev. A **66**, 052716 (2002).

Ariyasinghe W. M., Rad. Phys. Chem. **68**, 79 (2003).

Ariyasinghe W. M., Wickramarachi P., and Palihawadana P., Nucl. Instr. Meth. Phys. Res. B **259**, 841 (2007).

Baluja K. L., Jain A., Martino V. D., and Gianturco F. A., Europhys Lett. **17**, 139 (1992). Y. Jiang, J. Sun, and L. Wan Phys. Rev. A **52**, 398 (1995).

Becker K. H., McCurdy W., and Ornaldo T., work shop on *Electron Driven Processes: Scientific Challenges and Technological Opportunities* (March, 2000).

Bederson B. and Kiefer L. J., Rev. Mod. Phys. **43**, 601 (1971).

Blaauw H. J., Wagenaar R. W., Barends D. H., and de Heer F. J., J. Phys. B **13**, 359 (1980).

Bruche E., Ann. Phys. (Leipzing) **1**, 93 (1929).

Christophorou L. G., *Electron-Molecule Interactions and Their Applications* (Academic, Florida, 1984).

Christophorou L. G., Olthoff J. K., and Rao M. V. V. S., J. Phys. Chem. Ref. Data **25**, 1341 (1996).

Christophorou L. G., Olthoff J. K., and Rao M. V. V. S., J. Phys. Chem. Ref. Data **26**, 1 (1997).

Christophorou L. G. and Olthoff J. K., J. Phys. Chem. Ref. Data **27**, 1 (1998).

Christophorou L. G. and Olthoff J. K., J. Phys. Chem. Ref. Data **28**, 967 (1999).

Christophorou L. G. and Olthoff J. K., J. Phys. Chem. Ref. Data **30**, 449 (2001).

Christophorou L. G. and Olthoff J. K., App. Surf. Sci. **192**, 309 (2002).

Comstock AC-902, *Electro Static Analyzer Instruction Manual*, Comstock Inc., Oak Ridge, Tennessee.

Garcia G. and Manero F., Chem. Phys. Lett. **280**, 419 (1997).

Goains C. P., *Ph. D. Disser*tation, Baylor University, Waco, TX (2004).

Guo P., Ghebremedhin A., Ariyasinghe W. M., and Powers D., Phys. Rev. A **51**, 2117 (1995).

Iga I., Pinto P. R., and Homem M. G. P., *International Symposium on Electron-Molecule Collisions and Swarms, Tokyo* (1999).

Jiang Y., Sun J., and Wan L., Phys. Rev. A **62**, 062712 (2000).

Jin-Feng S., Bin X., Yu-Fang L., and De-Heng S., Chin. Phys. **14**, 1125 (2005).

Joshipura K. N. and Vinodkumar M., Pramana **47**, 57 (1996).

Kimball Physics EGG-3101, *Electron Gun Instruction Manual*, Kimball Physics Inc., Wilton, NH.

Makochekanwa C., Sueoka O., and Kimura M., *Gaseous Dielectrics X*, 181 (2004).

Makochekanwa C., Sueoka O., Kimura M., Kitajima M., and Tanaka H., Phys. Rev. A **71**, 032717 (2005).

Manero F., Blanco F., and Garcia G., Phys. Rev. A **66**, 032713 (2002).

MKS Baratron 626 A, *Capacitance Manometer Instructions Manual*, MKS Instruments, Andover, Massachusetts.

Nishimura H., *International Symposium on Electron-Molecule Collisions and Swarms, Tokyo* (1999).

Nishimura H., Nishimura F., Nakamura Y., and Okuda K., J. Phys. Soc. Jpn. **72**, 1080 (2003).

Nishimura H. and Nakamura Y., J. Phys. Soc. Jpn. **74**, 1160 (2005).

Nishimura H. and Hamada A., J. Phys. Soc. Jpn. **76**, 014301 (2007).

Sueoka O., Mori S., and Hamada A., J. Phys. B: At. Mol. Opt. Phys. **27**, 1453 (1994).

Sueoka O., Takaki H., Hamada A., Sato H., and Kumara M., Chem. Phys. Lett. **288**, 124 (1998).

Sueoka O., Makochekanwa C., and Kawate H., Nucl. Instr. Meth. Phys. Res. B 192, 206 (2002).

Szmytkowski C., Krzysztofowicz A. M., Janicki P., and Rosenthal L., Chem. Phys. Lett. **199**, 191 (1992).

Szmytkowski C., Mozejko P., Kasperski G., and Denga E. P., J. Phys. B: At. Mol. Opt. Phys. **33**, 15 (2000).

Tanaka H., Tachibana Y., Kitajima M., Sueoka O., Takaki H., Hamada A., and Kimura M., Phys. Rev. A **59**, 2006 (1999).

Trajmar S., Register D. F., and Chutjian A., *Electron Scattering by Molecules 2: Experimental Methods and Data*, (ELSEVIER SCIENCE BV, Amsterdam, 1983).

Zecca A., Karwaz G. P., and Brusa R., Phys. Rev. A **46**, 3877 (1992).